University of Nebraska - Lincoln
DigitalCommons@University of Nebraska - Lincoln

USDA National Wildlife Research Center - Staff Publications

U.S. Department of Agriculture: Animal and Plant Health Inspection Service

5-13-2019

Epidemic growth rates and host movement patterns shape management performance for pathogen spillover at the wildlife–livestock interface

Kezia R. Manlove
Utah State University, kezia.manlove@gmail.com

Laura M. Sampson
The Pennsylvania State University

Benny Borremans
University of California & Hasselt University

E. Frances Cassirer
Idaho Department of Fish and Game

Ryan S. Miller
Center for Epidemiology and Animal Health
See next page for additional authors

Follow this and additional works at: https://digitalcommons.unl.edu/icwdm_usdanwrc

Part of the Natural Resources and Conservation Commons, Natural Resources Management and Policy Commons, Other Environmental Sciences Commons, Other Veterinary Medicine Commons, Population Biology Commons, Terrestrial and Aquatic Ecology Commons, Veterinary Infectious Diseases Commons, Veterinary Microbiology and Immunobiology Commons, Veterinary Preventive Medicine, Epidemiology, and Public Health Commons, and the Zoology Commons

Manlove, Kezia R.; Sampson, Laura M.; Borremans, Benny; Cassirer, E. Frances; Miller, Ryan S.; Pepin, Kim M.; Besser, Thomas E.; and Cross, Paul C., "Epidemic growth rates and host movement patterns shape management performance for pathogen spillover at the wildlife–livestock interface" (2019). *USDA National Wildlife Research Center - Staff Publications*. 2283.
https://digitalcommons.unl.edu/icwdm_usdanwrc/2283

This Article is brought to you for free and open access by the U.S. Department of Agriculture: Animal and Plant Health Inspection Service at DigitalCommons@University of Nebraska - Lincoln. It has been accepted for inclusion in USDA National Wildlife Research Center - Staff Publications by an authorized administrator of DigitalCommons@University of Nebraska - Lincoln.

Authors

Kezia R. Manlove, Laura M. Sampson, Benny Borremans, E. Frances Cassirer, Ryan S. Miller, Kim M. Pepin, Thomas E. Besser, and Paul C. Cross

This article is available at DigitalCommons@University of Nebraska - Lincoln: https://digitalcommons.unl.edu/icwdm_usdanwrc/2283

PHILOSOPHICAL TRANSACTIONS B

royalsocietypublishing.org/journal/rstb

Research

Cite this article: Manlove KR, Sampson LM, Borremans B, Cassirer EF, Miller RS, Pepin KM, Besser TE, Cross PC. 2019 Epidemic growth rates and host movement patterns shape management performance for pathogen spillover at the wildlife–livestock interface. *Phil. Trans. R. Soc. B* **374**: 20180343. http://dx.doi.org/10.1098/rstb.2018.0343

Accepted: 13 May 2019

One contribution of 20 to a theme issue 'Dynamic and integrative approaches to understanding pathogen spillover'.

Subject Areas:
health and disease and epidemiology, ecology

Keywords:
pathogen spillover, wildlife–livestock interface, disease management, structured decision-making, disease model, dispersal kernel

Author for correspondence:
Kezia R. Manlove
e-mail: kezia.manlove@gmail.com

Electronic supplementary material is available online at https://dx.doi.org/10.6084/m9.figshare.c.4559240.

THE ROYAL SOCIETY PUBLISHING

Epidemic growth rates and host movement patterns shape management performance for pathogen spillover at the wildlife–livestock interface

Kezia R. Manlove[1], Laura M. Sampson[2], Benny Borremans[3,4], E. Frances Cassirer[5], Ryan S. Miller[6], Kim M. Pepin[7], Thomas E. Besser[8] and Paul C. Cross[9]

[1]Department of Wildland Resources and Ecology Center, Utah State University, Logan, UT 84321, USA
[2]Center for Infectious Disease Dynamics, Pennsylvania State University, University Park, PA 16802, USA
[3]Department of Ecology and Evolutionary Biology, University of California, Los Angeles, CA 90095-7239, USA
[4]Interuniversity Institute for Biostatistics and statistical Bioinformatics (I-BIOSTAT), Hasselt University, 3590 Diepenbeek, Belgium
[5]Idaho Department of Fish and Game, 3316 16th Street, Lewiston, ID 83501, USA
[6]United States Department of Agriculture, Animal and Plant Health Inspection Service, Center for Epidemiology and Animal Health, Fort Collins, CO 80523, USA
[7]National Wildlife Research Center, USDA-APHIS, Wildlife Services, 4101 Laporte Ave., Fort Collins, CO 80521, USA
[8]Department of Veterinary Microbiology and Pathology, Washington State University, Pullman, WA 99164-7040, USA
[9]U.S. Geological Survey, Northern Rocky Mountain Science Center, Bozeman, MT 59715, USA

KRM, 0000-0002-7200-5236; LMS, 0000-0001-8651-9302; BB, 0000-0002-7779-4107; KMP, 0000-0002-9931-8312; TEB, 0000-0003-0449-1989; PCC, 0000-0001-8045-5213

Managing pathogen spillover at the wildlife–livestock interface is a key step towards improving global animal health, food security and wildlife conservation. However, predicting the effectiveness of management actions across host–pathogen systems with different life histories is an on-going challenge since data on intervention effectiveness are expensive to collect and results are system-specific. We developed a simulation model to explore how the efficacies of different management strategies vary according to host movement patterns and epidemic growth rates. The model suggested that fast-growing, fast-moving epidemics like avian influenza were best-managed with actions like biosecurity or containment, which limited and localized overall spillover risk. For fast-growing, slower-moving diseases like foot-and-mouth disease, depopulation or prophylactic vaccination were competitive management options. Many actions performed competitively when epidemics grew slowly and host movements were limited, and how management efficacy related to epidemic growth rate or host movement propensity depended on what objective was used to evaluate management performance. This framework offers one means of classifying and prioritizing responses to novel pathogen spillover threats, and evaluating current management actions for pathogens emerging at the wildlife–livestock interface.

This article is part of the theme issue 'Dynamic and integrative approaches to understanding pathogen spillover'.

1. Introduction

Cross-species spillover of pathogens occurs when a pathogen that is released by a member of a reservoir host species goes on to establish and replicate in a different (recipient) host species [1–3]. While mitigating pathogen spillover and associated disease risk at the wildlife–livestock interface is a major goal for both human and animal health agencies [4], spillover management decisions

© 2019 The Author(s) Published by the Royal Society. All rights reserved.

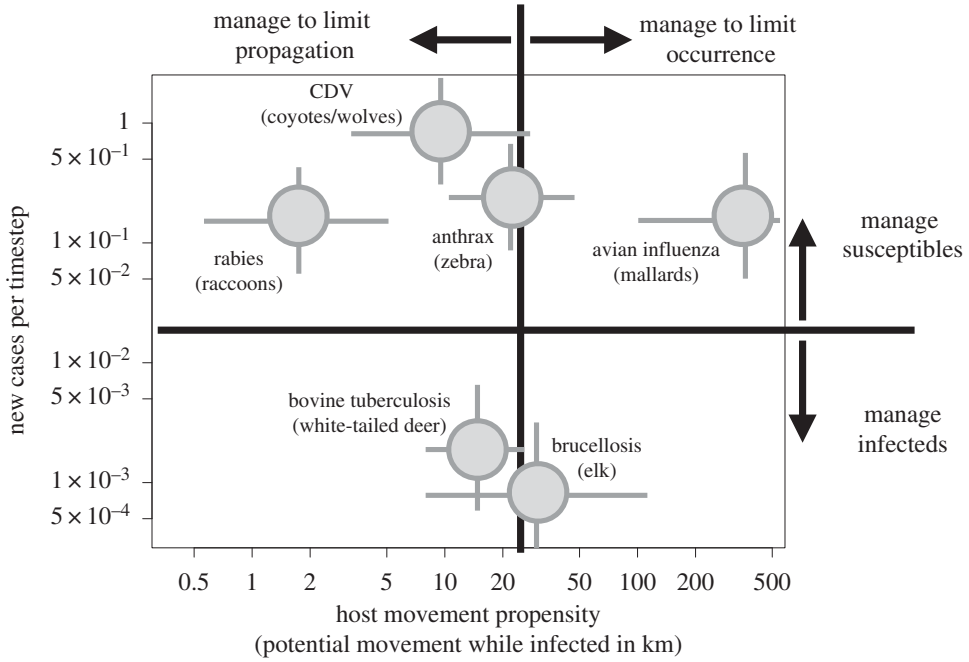

Figure 1. Hypothesized management efficacies across the pathogen propagation space. We partition pathogen propagation along two axes: epidemic growth rate and movement propensity of the reservoir host (here, quantified as typical number of kilometres moved during the infectious period). Relative performance of various management strategies is indicated with arrows outside the illustration's margins. Management actions that might fall into the upper left quadrant include local depopulation of either host at infected premises. Management in the upper right might include biosecurity measures targeting premises of either host, or prophylactic vaccination of the reservoir host. Management in the lower right could include a wide range of actions. Many actions might perform well in the relatively easily managed lower left-hand quadrant. System-specific values derived from a search of the empirical literature are indicated within the illustration. Values were left intentionally vague, and the values corresponding with the quadrant lines are arbitrarily chosen, since they will vary with ecological context, and with the particular organisms involved. Spatial extents indicated here are based on one important, current reservoir host listed beside each point. The upper bound of movement for avian influenza has been curtailed. See electronic supplementary material, table S1 for system-specific estimates. CDV references canine distemper virus.

are often context-specific and based on expert opinion [5]. In particular, there is limited scientific knowledge to guide management of spillover risk in understudied systems. Here, we propose a modelling framework designed to fill that gap by providing evidence-based guidance about optimal management over a wide range of ecological contexts.

A pathogen's spatial extent, and the spatial connectivity of the host populations, are critical drivers of disease management efficacy for many important wildlife–livestock [6] and wildlife–human spillover systems [7–9], and management of reservoir versus recipient hosts has been compared in some contexts [10]. However, spatially explicit two-host disease models have received less attention, with most published models describing management efficacy within a single-host species [11]. Moreover, these single-host models are often not intended to address spillover risk *per se*, but rather, to characterize dynamics leading up to or trailing after a spillover event.

Another group of models builds on the idea that spillover disease burdens depend on both the frequency and the consequences of individual spillover events. These 'multi-host' models often compare within- and between-species transmission rates to identify pathogens with a high risk of generating problematic spillover events [12–14]. Multi-host models have proven useful for characterising spillover rates, especially when merged with phylogenetic information specifically identifying the source of a given spillover event [15]. However, they are rarely extended to account for changing spillover risk as local reservoir prevalences vary through space and time (but see [16]).

Here, we explore how best to manage pathogen spillover and transmission in wildlife–livestock systems, using actions that are spatially explicit and could be applied to either the reservoir or the recipient host. Our model takes ideas previously employed for forecasting management performance in specific systems [17], but scales the approach up to apply across a wider range of host movement and epidemic growth rates. We start by justifying why a management-centred framework for wildlife–livestock spillover should explicitly incorporate movement. We then go on to describe a simple disease propagation model to characterise spillover risk and onward transmission across a wide range of hosts and pathogens. We next use the model to explore spillover management efficacies, and describe the patterns that the model produced. We end by discussing the limitations of this approach, and outlining features that could be added in the future.

2. Characterizing disease propagation in terms of epidemic growth rates and host movements

Our model is structured around three initial conjectures. First, we anticipate that the most efficient means of controlling pathogen spillover often rests on the spatial dynamics of the hosts. Hosts with high movement propensities can produce widespread spatial synchrony in spillover risk, making the precise location of future spillover events hard to predict [18]. In these cases, the best management option may be to target cross-species (i.e. interspecific) contacts by applying biosecurity measures or phytosanitary controls across a broad spatial extent [19]. When reservoir hosts move shorter distances, however, spatial containment in either the reservoir or the recipient host species (or both) may be possible.

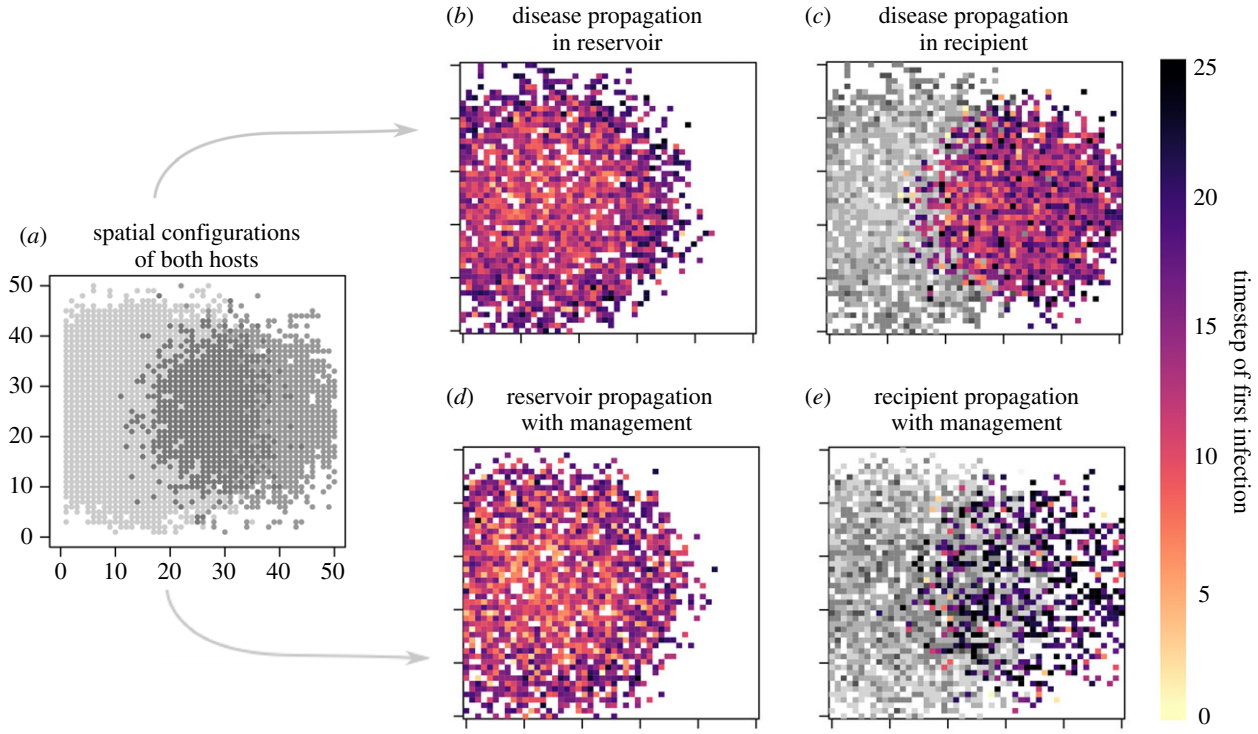

Figure 2. Simulation protocol. (*a*) Simulations begin by defining the spatial extent of the reservoir (light grey) and recipient (dark grey) hosts. A single infected individual is introduced into two reservoir host cells (*b*), with the structure of the subsequent epidemic determined by epidemic growth rate and host movement propensities. (*c*) The pathogen can then stochastically spill over to the recipient host in cells occupied by both host species (reservoir shown in grey; recipient in colour), at a rate determined by the interspecific contact rate and the pathogen's prevalence in the local reservoir host population. Management (here, retroactive vaccination of the recipient host) can alter the epidemic's progression in both host species (*d*,*e*). Management actions are compared in terms of their ability to minimize the epidemic's spatial extent in the recipient or reservoir host, and minimize the total number of recipient or reservoir host cases. Variation generated by manipulating spatial structure, local epidemic dynamics and management efficacy are shown in electronic supplementary material, figures S2–S4, respectively.

Second, we anticipate that the relative efficacies of various management actions will depend on how quickly an epidemic grows. If epidemic growth is rapid in the recipient host population, then depopulation or targeted vaccination at the time of the outbreak (here referred to as retroactive vaccination) may effectively limit post-spillover epidemic size. If epidemics grow slowly, actions like prophylactic vaccination or selective removal within the reservoir population may lower reservoir prevalence to the point where any cross-species spillover event becomes vanishingly rare (figure 1). Lastly, we expect that in some cases, many management actions will perform comparably. In these situations, relative economic and social costs of each action should factor heavily into management decision-making.

Testing these conjectures requires us to explicitly incorporate epidemic growth rates and host movement propensities into a model of epidemic spread. Like many single-host models [7], our model considers management in the context of a dynamic disease transmission process, but we make that process spatially explicit and allow new spillovers to emerge autonomously owing to underlying infection dynamics in the reservoir host. Like many multi-host models [13,14], magnitude of spillover risk is central to our model structure. However, where those models focus on the magnitude of risk in terms of force of infection from the reservoir host, we additionally focus on the spatial extent over which those events occur. Spatially linking both hosts in one model allows us to compare a wider range of management actions that span both host species.

3. Spillover simulation model

Our model includes three elements: transmission of the pathogen within a host species, transmission of the disease between species and movement of hosts across space. The model operates on a 50×50 grid of spatial cells. We assume that host population sizes are fixed and identical in all occupied cells. The model uses a deterministic SIR (susceptible–infected–recovered) disease process model with stochastic cell-to-cell host movements and between-species interactions to capture the effects of both host movement and epidemic growth.

Epidemic dynamics within a spatial cell follow the classic disease model of Kermack & McKendrick [20] without demography, which assumes that each individual's infection status transitions from susceptible (S) to infectious (I) to recovered (R). By keeping population sizes constant in all grid cells, we circumvent questions about whether within- and between-host-species transmission should be frequency- or density-dependent. During an epidemic's early exponential growth phase, the epidemic growth rate is equal to the difference between the transmission coefficient (β) and the recovery rate (γ) (electronic supplementary material, S2). We held recovery rate constant across all simulations and systematically altered epidemic growth rates by manipulating β alone (electronic supplementary material, figure S1A).

The model's spatial process starts with construction of an occupancy map for each host species, based on a stochastic selection of cells. The probability that a cell is occupied by a particular host species is determined with a draw from a symmetric, bivariate Gaussian kernel centred on that host's activity centre (i.e. surrounding a spatial centroid) and with a variance

Table 1. Management implementation within the model. The user-specified prevalence at which management began was varied systematically to take on values 0.001, 0.010, 0.100 and 1.00. S_{Reserv} and S_{Recip} reference the proportion of susceptible reservoir and recipient hosts, respectively; and I_{Reserv} and I_{Recip} refer to the proportion of infected reservoir hosts and recipient hosts, respectively. β is the transmission coefficient. N is the number of reservoir hosts per occupied cell and e_{ij} denotes the movement rate between the ith and jth cells. Throughout our simulations, we took a cell's neighbourhood to consist of all cells whose centroids were within three cell lengths of the target cell.

action	prevalence at which action begins	effect of action on system dynamics	action's spatial extent
biosecurity	user-specified	$\beta I_{Reserv} S_{Recip}$ becomes $\delta\beta I_{Reserv} S_{Recip}$ where $\delta \in (0, 1)$ is a multiplicative factor reducing β	neighbourhood of target cell
containment	user-specified	$e_{ij} = 1/10\,000$ when i and j are not on the same side of the containment boundary	all cells
depopulation	user-specified	I reset to 0 when depopulation occurs	neighbourhood of target cell
prophylactic vaccination	n.a.	S reset to $S(1 - \nu)$, where $\nu \propto N$/cell, the host's density within a cell	all cells
retroactive vaccination	user-specified	S reset to $S(1 - \nu)$, where $\nu = 1/R_0$, the herd immunity rate	neighbourhood of target cell
selective removal	user-specified	I_{Reserv} is reset to 0, and S_{Reserv} is proportionally increased	neighbourhood of target cell

equal to 50 (figure 2*a*). If a previously drawn cell is chosen a second time for the same species, we redraw from the same distribution until a set of 1000 unique cells is identified for each host (though both hosts can occupy the same cell). Spatial alignment between the host species is determined by the distance between host activity centres. This structure allows us to capture a gradient of spatial overlap between host species, from complete segregation to extensive spatial overlap throughout their ranges (electronic supplementary material, S4 and figure S2).

Individual reservoir and recipient hosts move stochastically between occupied grid cells at discrete time steps according to a tau-leap algorithm (electronic supplementary materials, S2.1). We assume that these movements have a negligible effect on cell population densities and hold population sizes constant within each occupied cell throughout the simulation. We only track the size of each disease compartment (namely, proportion of susceptible, infected and recovered individuals of each host species) within cells, not the disease status of particular individuals. Stochastic movement events by 'individual' infected animals spark dynamics within newly contacted cells, without altering cell densities. Movement rates are normalized so that the same number of cell-to-cell movements is expected in all simulations, but the structure of these movements varies controllably: movements are drawn from a monotonically decreasing function of Euclidean distance between cell centroids (i.e. a movement kernel; electronic supplementary material, S2.2) and we control host movement patterns by manipulating the distribution of movement distances (which we refer to as the host's 'movement propensity'). The probability that a dispersing host is infected is proportional to the local prevalence in that host's population. Movement kernels with heavy tails correspond to high-dispersal systems (high movement propensity), while movement kernels with light tails correspond to low-dispersal (low movement propensity) systems (electronic supplementary material, figure S1B). Note that larger values of c, the parameter controlling tail weight, correspond to lighter tails (electronic supplementary material, figure S1B). Epidemics simulated under high movement propensities seed more new infections at a distance than epidemics arising under lower movement propensities [21], facilitating faster spatial spread. For simplicity, we apply the same dispersal kernel to both host species in all simulations presented here, and we do not allow colonization of unoccupied cells. Arrival of a single infected host in an uninfected host cell always and instantly sparks a local epidemic in the newly contacted cell (figure 2*b*).

Contacts between reservoir and recipient hosts are also treated as stochastic. The number of interspecific contacts is based on a pre-specified interspecific contact rate, which is held constant across all simulations. Contacts are then randomly assigned across all cells occupied by both reservoir and recipient hosts. The probability that an interspecific contact involves an infected reservoir host is proportional to the current infection prevalence in that cell's reservoir host population. Though reservoir-to-recipient contacts are required to initiate epidemic dynamics in the recipient host population, we assume that recipient host populations experience no additional force of infection from reservoir hosts in local or neighbouring cells following the initial spillover event (figure 2*c*). Stochastic movements between cells populated with recipient hosts can then allow the epidemic to propagate throughout the entire recipient host population.

(a) Management actions

Our investigation focused on six forms of management: prophylactic vaccination applied across an entire population regardless of current disease status, retroactive vaccination applied to infected cells and their neighbours following detection of disease, contact biosecurity, depopulation, spatial containment and selective removal of infected reservoir hosts (figure 2*d*,*e*). Details on the implementation of all management actions within the model are contained in table 1 and electronic supplementary material, S2.3. In all

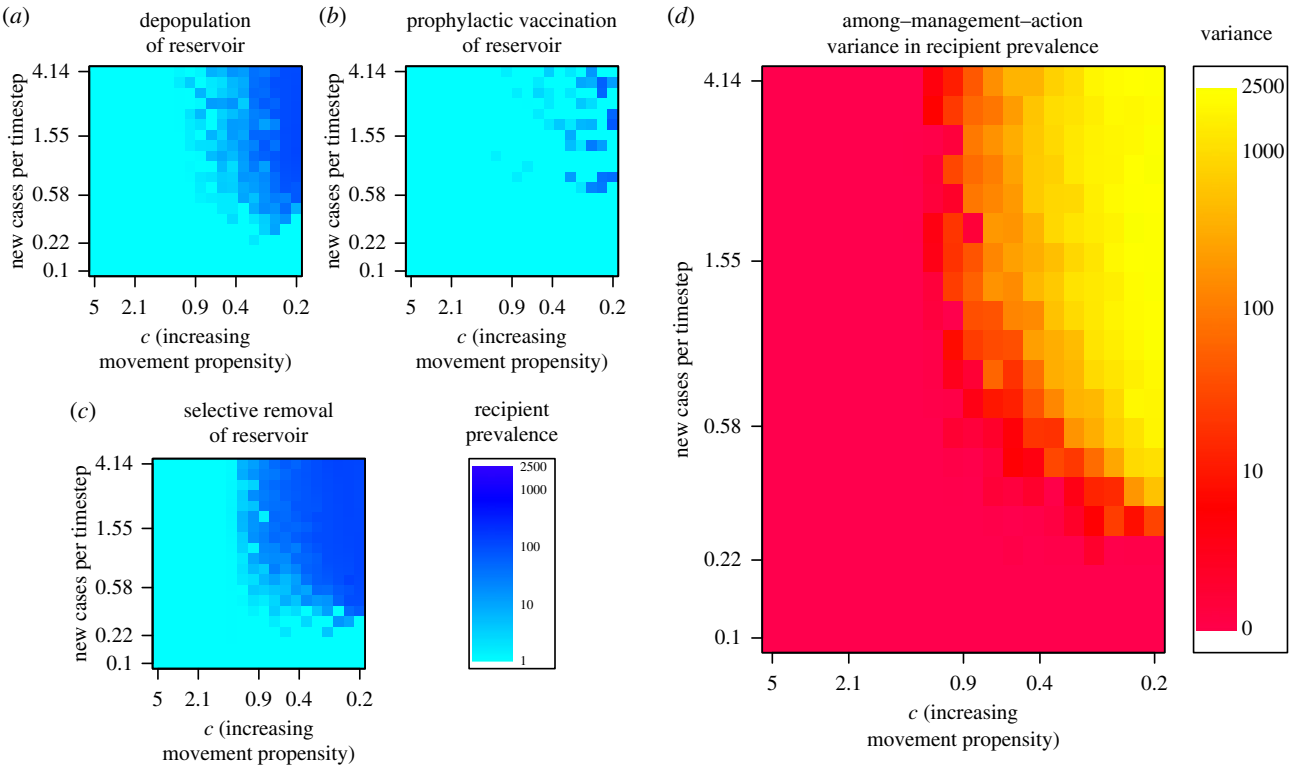

Figure 3. Simulation output. Heat maps (*a*–*c*) show the aggregate recipient host prevalence under three different management actions along the dimensions of epidemic growth rate (cases per timestep) and movement distance (movement propensity increases to the right): (*a*) depopulation of the reservoir host; (*b*) prophylactic vaccination of the reservoir host; and (*c*) selective removal of the reservoir host. In cases where unmanaged epidemics were large, outcomes varied dramatically among management actions and a clear 'best action' was identifiable (this is the case among the three sets of actions shown here, in which prophylactic vaccination of the reservoir clearly outperforms the other two actions for the fastest-growing, fastest-spreading epidemics). However, in cases where unmanaged epidemics were small, many actions performed comparably and the variance in recipient prevalence among actions was low (*d*). Variance among management outcomes increased with both movement and the number of cases per timestep. Simulations in (*a*–*c*) partition both epidemic growth rate and host movement propensity into 20 blocks, fix management initiation prevalence to 0.01 and set the spatial divide between host centroids to 30 cells. (Online version in colour.)

cases except for prophylactic vaccination, management was applied only to cells exceeding a specified threshold prevalence in the reservoir host (and to the direct neighbours of those cells for retroactive vaccination and depopulation; table 1).

This management structure leaves ample room for further development, including exploration of cost constraints and more complex management schemes. However, adding more detail would require tailoring the model to a specific system, so here we simply present the overarching structure and leave further specification to future work.

(b) Model process and outputs

We initiated the simulation by introducing the pathogen into two randomly chosen reservoir host cells at timestep 1, and simulated the epidemic forward for 60 timesteps. We recorded the time of first infection separately for reservoir and recipient hosts at each cell. Once a cell was infected, future pathogen introductions did not alter local epidemic dynamics. After the simulation, we calculated the proportion of reservoir and recipient host cells that became infected, along with the aggregate prevalence (which we calculated as the sum of infections in all cells at all timesteps) over the full simulation. These metrics—spatial extent of the reservoir and recipient host epidemics, along with maximum epidemic size and total disease-induced mortalities in both hosts—provided a basis for comparing disease propagation dynamics under varying rates of host movement and epidemic growth. The model was implemented as a de novo simulation in R [22].

4. Identifying the most effective management strategies

In order to identify which management action produced the best results under particular conditions of host movement propensities and epidemic growth, we ran simulations across a gridded version of the parameter space (electronic supplementary material, S3 and table S1). Parameters varied along the following six dimensions: (i) epidemic growth rate; (ii) variance and kurtosis of the hosts' dispersal function ('movement propensity'); (iii) prevalence at which management began; (iv) host density within each cell; (v) distance between reservoir and recipient host activity centres; and (vi) management objective of interest. The objectives we considered were minimizing spatial extent of the epidemic in the recipient host; minimizing total number of recipient host cases; minimizing spatial extent of the epidemic in the reservoir host; or minimizing total number of reservoir host cases. We focus primarily on spillover management in the recipient host population, but include results from objectives focused on the reservoir host in electronic supplementary material, S5.4.

We first explored raw output values over the disease propagation space (figure 3) and then tabulated which management action performed 'best' (i.e. minimized epidemic size or

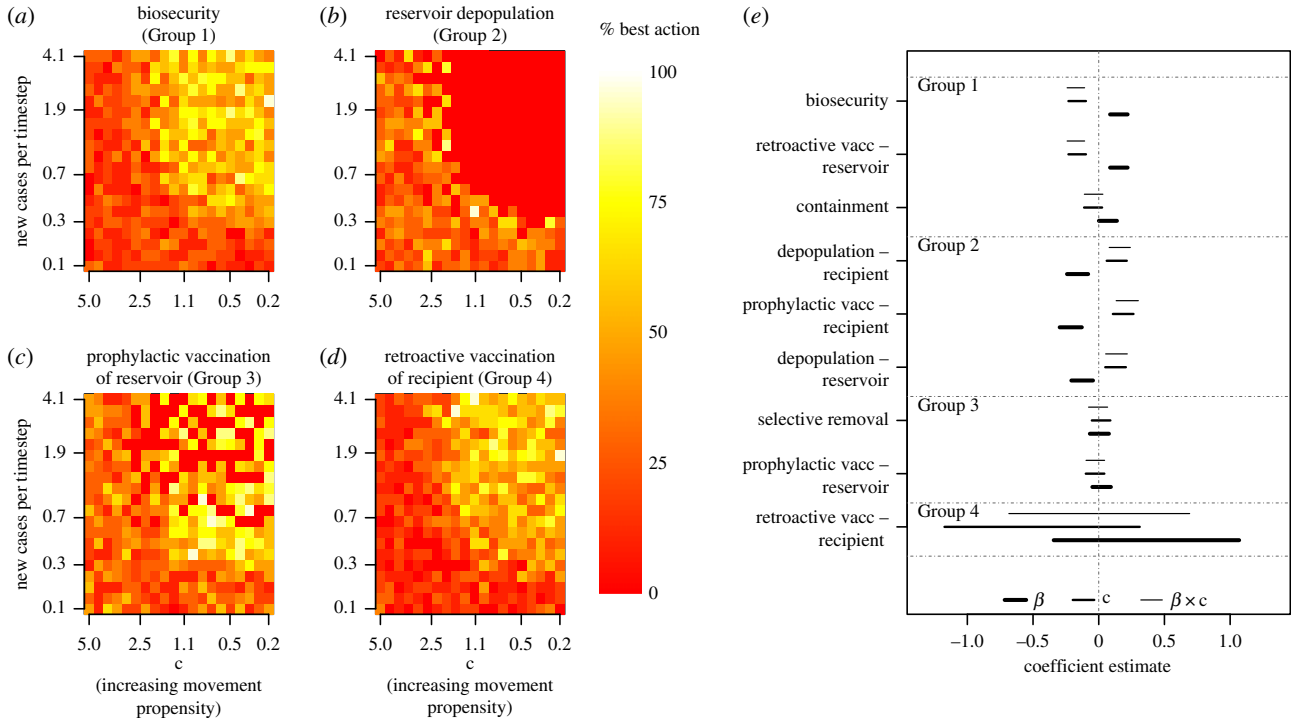

Figure 4. Comparison of management actions over the disease propagation space. (*a–d*) Relative performances of four representative management actions at controlling spillover (measured here in terms of the total number of recipient host patches infected) across the parameter space. Pixel colours represent the raw proportion of times that the action performed better than all other actions at that particular combination of epidemic growth rate and movement propensity. (*e*) Coefficient estimates for the relationship between epidemic growth rate (β; thickest lines), movement propensity (*c*; medium-width lines) and the β-by-*c* interaction (finest lines) from logistic regression models describing when each management action performed best. Positive coefficient estimates for β indicate that the action's performance improved relative to other actions as epidemic growth rate increased. Positive coefficient estimates for (*c*) indicate that the action's performance improved relative to other actions as host movement propensity declined. Positive coefficient estimates for the β-by-*c* interaction indicate that the action's relative performance improved when epidemic growth rates were high, but host movement propensities were low. Lines show 95% confidence intervals around each point estimate. Parallel results for the other three objectives are shown in electronic supplementary material, figures S6–S8, and additional details on the underlying simulations are included in electronic supplementary material, S5.1 and S5.3. (Online version in colour.)

epidemic spatial extent in the reservoir or recipient host) at every parameter combination (figure 4*a–d*). We then used logistic regression to correlate when a management action was ranked as the best (yes or no), with epidemic growth rate and tail weight in the host's dispersal kernel. All simulations contributed to model fits, so that inferences were balanced over a range of values for reservoir population density, spatial divide between host activity centres and prevalence at which management began. Finally, we grouped management actions according to their coefficient estimates from the logistic regression (figure 4) and compared conditions of strong relative performance for each group to our expectations in figure 1.

5. Results

Our simulator produced a wide range of spatio-temporal spillover and transmission dynamics (figure 3; electronic supplementary material, figures S3 and S4) and these dynamics generally responded as expected to the various management interventions (figure 3; electronic supplementary material, figure S5). While the results presented here focus on one objective, limiting the total number of infected cells in the recipient host population, similar patterns were observed for limiting the total number of recipient hosts infected (electronic supplementary material, S5.3). Unsurprisingly, we saw some deviations from these patterns when objectives were centred on the reservoir host. For instance, we allowed biosecurity to only target interspecific contacts, so it had no bearing on disease dynamics in the reservoir host. Most of the observed deviations between the reservoir and recipient host objectives could be readily explained with similar logic.

Action performances typically fell into two groups when aggregated across the entire parameter space, but which actions fell into which group depended on objective (electronic supplementary material, table S3). When the objective was minimizing the epidemic's spatial extent in the recipient host population, the better-performing group consisted of biosecurity, prophylactic vaccination of the reservoir host, and retroactive vaccination of either host (electronic supplementary material, table S3). Epidemics tended to be easily controlled by many management strategies when movements were mostly local and epidemic growth rates were low (figure 3; see electronic supplementary material, S5.2 and S5.3 for statistical results, and S5.4 for results under other objectives).

Actions could be grouped according to how their relative performance related to epidemic growth rate and host movement propensities (figure 4). Biosecurity, containment and retroactive vaccination of the local reservoir host (Group 1), which all aim to limit spillover effects by controlling interspecific contact or spatial propagation, performed best for fast-growing epidemics in hosts with high movement propensities (the upper right-hand corner of figure 1). Depopulation of both hosts, along with prophylactic vaccination of the recipient host (Group 2) had the strongest

relative performance in scenarios where epidemics grew quickly, but host movement propensities were low. The relative performance of selective removal and prophylactic vaccination of the reservoir (Group 3), both of which target prevalence and epidemic growth rates in the reservoir population, did not change substantially with changes in epidemic growth rate or host movement propensities. The groupings of management actions that performed similarly depended on the objective function, and this was particularly true when the measured objective focused on a different host. For instance, when the objective was to minimize infected reservoir (as opposed to recipient) patches, selective removal performed best when epidemics grew slowly, whereas prophylactic vaccination of the reservoir was best when epidemic growth rates were high, even though these actions were grouped together when the objective was to minimize epidemic size or extent in the recipient host (electronic supplementary material, figure S7).

6. Discussion

Pathogen spillover at the wildlife–livestock interface is a persistent and expensive problem for food security and wildlife conservation alike. While pathogen spillover dynamics have been explicitly studied in many wildlife–livestock systems, disease ecologists lack a general framework for considering the context in which each management action should perform best. Here, we presented a framework for forecasting management performance of spatiotemporally explicit spillover events.

Our simulation results usually agreed with our *a priori* intuition about how management would interact with spatially explicit epidemic propagation. Epidemic growth rate and host movement propensity interacted to generate variation in epidemic size and spatial extent (figure 4; electronic supplementary material, figures S6–S8) and epidemic growth rate was generally the most powerful determinant of which management action performed 'best' (figure 4*e*; see electronic supplementary material, S5.4 for additional results). While our findings are likely sensitive to the range of parameter values explored (epidemics sometimes failed to propagate in one or both hosts in a substantial region of the parameter space), they were nevertheless consistent with the basic categorization proposed in figure 1. In fast-growing, high-movement-propensity systems, limiting and localizing recipient host interactions with infected reservoir hosts—whether by reducing reservoir prevalence through vaccination, or by reducing interspecific contact rates through biosecurity—was the best strategy for recipient-focused objectives. Containment of the reservoir host also performed relatively well in these scenarios, except in cases where host movements consistently exceeded the size of the containment region (though the implications of varying containment region size were not explored here). Actions like depopulation of either host species or prophylactic vaccination of the recipient host, which limit epidemic growth by controlling the size of the susceptible pool without targeting movement, performed relatively better when epidemic growth rates were high and movement propensities were low. These actions might be favoured for fast-growing, low-movement-propensity epidemics, and may be competitive in higher-movement-propensity scenarios, depending on cost. Performance of actions that controlled local prevalence in reservoir host populations through prophylactic vaccination or selective removal within the reservoir population did not exhibit strong patterns with epidemic growth rate or host movement propensities. However, retroactive vaccination of the reservoir host performed comparably in the same ecological scenarios, and may be more politically and socially palatable when feasible (electronic supplementary material, table S3; [23]).

All management actions were competitive with one another when epidemic growth rates were slow, clearing a path for cost to play a larger role in decision-making (figure 3*d*). This partially held for fast-growing epidemics with low host movement propensities as well, and has been demonstrated in detail in several wildlife–livestock spillover systems. For instance, management models of foot-and-mouth disease (which we might categorize as a fast-growing disease with a lower host movement propensity) have investigated a wide range of different management strategies and found that a variety of actions might be deemed appropriate, depending on the specific objective, the action's cost and the prevalence at which management begins [24,25].

Contrary to our initial expectations, the tail weight of the dispersal kernel did not play a particularly powerful role in shaping management efficacy throughout our simulations (figure 4*e*). This could be because we held the total number of cell-to-cell movements constant throughout the simulations. In reality, host species vary in both the number and the distance of moves they make, as well as their local densities, and this has been shown to have substantial impacts on local epidemic growth in some cases (e.g. [26]). We anticipate that movement may thus play a more powerful role than these results suggest, but this question merits additional follow-up.

We elected to emphasize epidemic growth rate instead of the pathogen's basic reproductive ratio (R_0) because disease management depends on calendar time rather than the pathogen's generational timespan. Management requiring construction of fencing for biosecurity, or depopulation of infected premises, would be much more effective in a system with a slow epidemic growth rate than a rapid one, even if the epidemics were identical in terms of R_0. This could play out empirically, for example, in bovine tuberculosis (bTB) management in Michigan, USA, where models suggest that a relatively constant, but low level of spillover pressure from wildlife could be successfully mitigated through fencing [27]. It is the slow growth rate, and not that the basic reproductive ratio, that renders fencing feasible for Michigan bTB. Similarly, slow measures would be less effective for a pathogen with a comparable R_0 (estimated to be around 1.5 for Michigan bTB), but a shorter infectious period.

(a) Framework limitations

This model was designed around the assumptions most relevant to our particular question of interest, namely, how allocation of disease management effort should vary along a two-dimensional continuum of epidemic growth rate and host movement propensity. Many other facets of the pathogen spillover and management decision-making process were simplified to isolate this question. In particular, the disease process model is subject to the same constraints facing many SIR models: we assumed that immunity is lifelong; that disease does not induce mortality; that host densities are constant through space and time; and that disease-related rates like recovery and transmission are effectively constant

across all individuals. Additionally, our selection of timescale and epidemic duration was arbitrary. We assumed that host movements were random and independent, and that both host species moved according to the same movement kernels. All of these assumptions are unrealistic in some scenarios, and we discuss each in greater depth in electronic supplementary materials, S6.

Additionally, our results are driven in part by the assumed efficacy of each management action. Efficacy values were generated from a set of preliminary simulations identifying parameter values that generated similar effect sizes. A full sensitivity analysis incorporating all model parameters is beyond our current scope; however, we recognize that such a study is a critical next-step. A simplified tactic, in which we sample randomly over an ungridded (but uniform) parameter space to assess output sensitivities of the various parameters, is the subject of current investigation. At this time, we simply emphasize that our objectives in querying this model are also fundamentally different from those of a researcher aiming to forecast management efficacy specific to a particular system. A more detailed investigation of sensitivities to cost, efficacy, etc. would be important when comparing management options for specific systems where the general process parameter space is already quite constrained.

We only allowed for a single management action to be undertaken at a time, and we do not account for costs or logistical constraints associated with those actions. Costs vary dramatically across systems and contexts (see, for example, the discussion in [28] surrounding the costs of brucellosis management), and placing any specific cost on an action quickly constrains the set of systems to which the results extend. At the same time, cost–benefit trade-offs are already being used to justify spillover disease management in reservoir hosts. For example, Sterner *et al*. [29] argue that even though oral rabies vaccination in the USA and Canada is quite costly, those aggregate costs are lower than the costs of post-exposure prophylaxis that would be required to manage rabies in the spillover host (here, humans). Further comparative inquiry into cost is increasingly necessary.

Beyond economic costs, disease management logistics take time to coordinate, and this constrains how quickly management follows detection and how many cells can be managed at once. From a political stance, reservoir and recipient host management decisions are often determined by separate agencies with distinct, and sometimes discordant, objectives. Being able to weigh disease management actions against more complex objective functions that include those different viewpoints is an important extension that would allow managers, researchers, livestock producers and conservationists to reach some common ground.

Finally, our model does not allow management actions to fundamentally alter the system's underlying ecology (i.e. to pull 'ecological levers' [23]). In reality, some of these actions—in particular, depopulation and selective removal—have the potential to impose major and lasting alterations. Allowing management to perturb underlying system ecology is an important issue for future exploration.

(b) Framework extensions

The model's simple structure means it can generate initial expectations about epidemic progression in understudied systems, even before the specific epidemiological process is well understood. Accounting for disease and movement dynamics in both reservoir and recipient hosts allows us to compare a broader suite of management actions available for constraining emerging pathogens. Rapid parameterization of the model may often be feasible, since both epidemic growth rate and host movement structure can be inferred from data available shortly after an epidemic's inception. As system-specific information accumulates, the modelling structure could be refined to encapsulate emerging detail about how, when and where to optimally manage the system [6,30].

If multiple management options are available, coupling actions that tackle different aspects of transmission (e.g. actions from contrasting groups in figure 4) may be beneficial. For instance, reservoir-focused actions can reduce the overall spillover risk by limiting the spatial extent and prevalence of the pathogen in the reservoir. However, unless these actions completely eliminate spillover risk, they may be most effective when coupled with targeted, responsive management in the recipient host (e.g. depopulation or retroactive vaccination). This both-hosts approach has already been used to manage several slow-growing, low-movement-propensity pathogens at the wildlife–livestock interface (e.g. brucellosis management around the Greater Yellowstone Ecosystem [31], or bovine tuberculosis management in Minnesota, USA white-tailed deer [32]).

Lastly, the best-performing management in any context also depended on the objective. This is consistent with a rich body of work on adaptive management and structured decision-making in a range of ecological contexts [33] including disease dynamics [24,34]. In reality, objectives likely differ for the two host species, with recipient management focusing around limiting aggregate case load, and reservoir management emphasizing detection and mitigation of prevalence pulses [18]. Given the extensive discussion of objective functions elsewhere, however, we do not dwell on them further here.

7. Conclusion

The risk and burden of pathogen spillover depends on a spatially explicit disease propagation process that operates in both reservoir and recipient host populations. Our model provides a useful starting point for planning management of disease at the wildlife–livestock interface based on general epidemiological traits of the system. It underscores the critical role that epidemic growth rate and spatial context play in determining management efficacy, and could be tailored to the specifics of a wide variety of pathogen spillover systems.

Data accessibility. All estimates included in figure 1 are tabled in the electronic supplementary material files, and simulation and analysis code are contained in the electronic supplementary material.

Authors' contributions. K.R.M. and P.C.C. developed the conceptual framework and all authors contributed to model refinements. K.R.M. and L.M.S. constructed the simulation model, and K.R.M., L.M.S. and P.C.C. developed the model analysis. K.R.M. drafted the manuscript and all authors contributed to multiple rounds of manuscript revision.

Competing interests. We have no competing interests.

Funding. L.M.S. was supported by the L'Oreal For Women in Science Fellowship. K.M.P. was supported by USDA.

Disclaimer. Any use of trade, firm or product names is for descriptive purposes only and does not imply endorsement by the US Government.

References

1. Power AG, Mitchell CE. 2004 Pathogen spillover in disease epidemics. *Am. Nat.* **164**, S79–S89. (doi:10.1086/424610)
2. Pulliam JR. 2008 Viral host jumps: moving toward a predictive framework. *EcoHealth* **5**, 80. (doi:10.1007/s10393-007-0149-6)
3. Plowright RK, Parrish CR, McCallum H, Hudson PJ, Ko AI, Graham AL, Lloyd-Smith JO. 2017 Pathways to zoonotic spillover. *Nat. Rev. Microbiol.* **15**, 502–510. (doi:10.1038/nrmicro.2017.45)
4. World Health Organization (WHO), Food and Agriculture Organization of the United Nations (FAO) & World Organisation for Animal Health (OIE). 2004 Report of the WHO/FAO/OIE joint consultation on emerging zoonotic diseases, 3 to 5 May, Geneva. Geneva, Switzerland: WHO.
5. Joseph MB, Mihaljevic JR, Arellano AL, Kueneman JG, Preston DL, Cross PC, Johnson PT. 2013 Taming wildlife disease: bridging the gap between science and management. *J. Appl. Ecol.* **50**, 702–712. (doi:10.1111/1365-2664.12084)
6. Probert WJ *et al*. 2018 Real-time decision-making during emergency disease outbreaks. *PLoS Comput. Biol.* **14**, e1006202. (doi:10.1371/journal.pcbi.1006202)
7. Fraser C, Riley S, Anderson RM, Ferguson NM. 2004 Factors that make an infectious disease outbreak controllable. *Proc. Natl Acad. Sci. USA* **101**, 6146–6151. (doi:10.1073/pnas.0307506101)
8. Riley S, Ferguson NM. 2006 Smallpox transmission and control: spatial dynamics in Great Britain. *Proc. Natl Acad. Sci. USA* **103**, 12 637–12 642. (doi:10.1073/pnas.0510873103)
9. Riley S. 2007 Large-scale spatial-transmission models of infectious disease. *Science* **316**, 1298–1301. (doi:10.1126/science.1134695)
10. Iacono GL *et al*. 2015 Using modelling to disentangle the relative contributions of zoonotic and anthroponotic transmission: the case of Lassa fever. *PLoS Neg. Trop. Dis.* **9**, e3398. (doi:10.1371/journal.pntd.0003398)
11. Lloyd-Smith JO, George D, Pepin KM, Pitzer VE, Pulliam JR, Dobson AP, Hudson PJ, Grenfell BT. 2009 Epidemic dynamics at the human–animal interface. *Science* **326**, 1362–1367. (doi:10.1126/science.1177345)
12. Haydon DT, Cleaveland S, Taylor LH, Laurenson MK. 2002. Identifying reservoirs of infection: a conceptual and practical challenge. *Emerg. Infect. Dis.* **8**, 1468–1473. (doi:10.3201/eid0812.010317)
13. Fenton A, Pedersen AB. 2005. Community epidemiology framework for classifying disease threats. *Emerg. Infect. Dis.* **11**, 1815. (doi:10.3201/eid1112.050306)
14. Viana M, Mancy R, Biek R, Cleaveland S, Cross PC, Lloyd-Smith JO, Haydon DT. 2014 Assembling evidence for identifying reservoirs of infection. *Trends Ecol. Evol.* **29**, 270–279. (doi:10.1016/j.tree.2014.03.002)
15. Mather AE *et al*. 2013 Distinguishable epidemics of multidrug-resistant *Salmonella* Typhimurium DT104 in different hosts. *Science* **341**, 1514–1517. (doi:10.1126/science.1240578)
16. Washburne AD, Crowley DE, Becker DJ, Manlove KR, Childs ML, Plowright RK. 2019 Percolation models of pathogen spillover. *Phil. Trans. R. Soc. B* **374**, 20180331. (doi:10.1098/rstb.2018.0331)
17. Tildesley MJ, Bessell PR, Keeling MJ, Woolhouse ME. 2009 The role of pre-emptive culling in the control of foot-and-mouth disease. *Proc. R. Soc. B* **276**, 3239–3248. (doi:10.1098/rspb.2009.0427)
18. Plowright RK, Becker DJ, McCallum H, Manlove KR. 2019 Sampling to elucidate the dynamics of infections in reservoir hosts. *Phil. Trans. R. Soc. B* **374**, 20180336. (doi:10.1098/rstb.2018.0336)
19. Shriner SA *et al*. 2016 Surveillance for highly pathogenic H5 avian influenza virus in synanthropic wildlife associated with poultry farms during an acute outbreak. *Sci. Rep.* **6**, 36237. (doi:10.1038/srep36237)
20. Kermack WO, McKendrick AG. 1927 A contribution to the mathematical theory of epidemics. *Proc. R. Soc. A* **115**, 700–721. (doi:10.1098/rspa.1927.0118)
21. Hallatschek O, Fisher DS. 2014 Acceleration of evolutionary spread by long-range dispersal. *Proc. Natl Acad. Sci. USA* **111**, E4911–E4919. (doi:10.1073/pnas.1404663111)
22. R Core Team. 2017 *R: A language and environment for statistical computing*. Vienna, Austria: R Foundation for Statistical Computing. See https://www.R-project.org/.
23. Sokolow SH *et al*. 2019 Ecological interventions to prevent and manage zoonotic pathogen spillover. *Phil. Trans. R. Soc. B* **374**, 20180342. (doi:10.1098/rstb.2018.0342)
24. Li S-L, Bjørnstad ON, Ferrari MJ, Mummah R, Runge MC, Fonnesbeck CJ, Tildesley MJ, Probert WJ, Shea K. 2017 Essential information: uncertainty and optimal control of Ebola outbreaks. *Proc. Natl Acad. Sci. USA* **114**, 5659–5664. (doi:10.1073/pnas.1617482114)
25. Probert WJ *et al*. 2016 Decision-making for foot-and-mouth disease control: objectives matter. *Epidemics* **15**, 10–19. (doi:10.1016/j.epidem.2015.11.002)
26. Tildesley MJ, Keeling MJ. 2009 Is R0 a good predictor of final epidemic size: foot-and-mouth disease in the UK. *J. Theo. Biol.* **258**, 623–629. (doi:10.1016/j.jtbi.2009.02.019)
27. Wilber MQ, Pepin KM, Campa III H, Hyngstrom SE, Lavelle MJ, Xifara T, VerCauteren K, Webb CT. 2019 Modeling multi-species and multi-mode contact networks: implications for persistence of bovine tuberculosis at the wildlife–livestock interface. *J. Appl. Ecol.* **56**, 1471–1481. (doi:10.1111/1365-2664.13370)
28. Boroff K, Kauffman M, Peck D, Maichak E, Scurlock B, Schumaker B. 2016 Risk assessment and management of brucellosis in the southern greater Yellowstone area (II): cost–benefit analysis of reducing elk brucellosis prevalence. *Prev. Vet. Med.* **134**, 39–48. (doi:10.1016/j.prevetmed.2016.09.025)
29. Sterner RT, Meltzer MI, Shwiff SA, Slate D. 2009 Tactics and economics of wildlife oral rabies vaccination, Canada and the United States. *Emerg. Infect. Dis.* **15**, 1176. (doi:10.3201/eid1508.081061)
30. Carpenter TE, O'Brien JM, Hagerman AM, McCarl BA. 2011 Epidemic and economic impacts of delayed detection of foot-and-mouth disease: a case study of a simulated outbreak in California. *J. Vet. Diag. Invest.* **23**, 26–33. (doi:10.1177/104063871102300104)
31. Scurlock BM, Edwards WH, Cornish T, Meadows L. 2010 Using test and slaughter to reduce prevalence of Brucellosis in elk attending feedgruonds in the Pinedale elk herd unit of Wyoming; results of a 5 year pilot project, Wyoming Game and Fish Department, Cheyenne, Wyoming.
32. Carstensen M, O'Brien DJ, Schmitt SM. 2011 Public acceptance as a determinant of management strategies for bovine tuberculosis in free-ranging US wildlife. *Vet. Microbiol.* **151**, 200–204. (doi:10.1016/j.vetmic.2011.02.046)
33. Martin J, Runge MC, Nichols JC, Lubow BC, Kendall WL. 2009 Structured decision making as a conceptual framework to identify thresholds for conservation and management. *Ecol. Appl.* **19**, 1079–1090. (doi:10.1890/08-0255.1)
34. Wasserberg G, Osnas EE, Rolley RE, Samuel MD. 2009 Host culling as an adaptive management tool for chronic wasting disease in white-tailed deer: a modelling study. *J. Appl. Ecol.* **46**, 457–466. (doi:10.1111/j.1365-2664.2008.01576.x)

Epidemic growth rates and host movement patterns shape management performance for pathogen spillover at the wildlife-livestock interface

K. R. Manlove, L. M. Sampson, B. Borremans, E. F. Cassirer, R. S. Miller,
K. M. Pepin, T. E. Besser, P. C. Cross*

April, 2019

Contents

Disclaimer: This draft manuscript is distributed solely for the purposes of scientific peer review. Its content is deliberative and predecisional, so it must not be disclosed or released by reviewers. Because the manuscript has not yet been approved for publication by the U.S. Geological Survey (USGS), it does not represent any official USGS finding or policy.

1 Empirical estimates of epidemiological rates

Disease	**Exponential growth rate**	β	γ	**Potential movement while infected (km)**
Brucellosis	0.0006 [1]	NA	NA	3-8 km/y [2]
Bovine Tuberculosis	0.002 ($R_0 \approx 2.59$ [3])	NA	NA	15 6km/y [4]
Rabies	0.152; $R_0 \approx$ 2-2.44 [3,5]	0.18	35	3km [6]
Avian influenza	0.18; $R_0 \approx 2.24$ [7,8]	0.0078 [9]	7d [10]	584-712 km [11]
Canine distemper (CDV)	0.42	0.16-0.30 [12]	15-23d acute; 67-74d persistent [12,13]	17.3 km (based on a mean pack range size of 300km^2) [14]
Anthrax	0.46; $R_0 \approx$ 2.98-5.97 [15]	22.5	7.5 d [16]	3 km/d

Table S1: Estimated epidemic growth rates and host movement potentials for systems shown in Figure 1 of the main text. Undoubtedly, an SIR process model is insufficient for any one of these systems. However, SIR-based estimates may still be sufficient for the coarse classification we aim to make on the simple basis of epidemic growth rate and host movement.

2 Model structure

The model begins with a spatial grid of 50x50 cells that could approximate counties in the U.S. (we envision 30mi x 30mi grid cells, but the exact spatial extent of the cells does not affect the simulations). The disease process within each cell follows the model of Kermack and McKendrick (1927). This model rests on a set of three ordinary differential equations (ODEs) describing how individuals within a population move from Susceptible (S) to Infected (I) to recovered

(R) states.

$$\frac{dS}{dt} = -\beta SI \tag{1}$$

$$\frac{dI}{dt} = \beta SI - \gamma I \tag{2}$$

$$\frac{dR}{dt} = \gamma I \tag{3}$$

The epidemic growth rate can be determined by using the Jacobian of the set of ODEs, solved at state values corresponding to the disease-free equilibrium. The Jacobian of the ODEs is simply the derivative of each equation in the set with respect to each variable. Here,

$$J = \begin{bmatrix} -\beta I^* & -\beta S^* & 0 \\ \beta I^* & \beta S^* - \gamma & 0 \\ 0 & \gamma & 0 \end{bmatrix} \tag{4}$$

Thus,

$$\det(\mathbf{J} - \mathbf{\Lambda I}) = \begin{vmatrix} -\beta I^* - \Lambda & -\beta S^* & 0 \\ \beta I^* & \beta S^* - \gamma - \Lambda & 0 \\ 0 & \gamma & 0 - \Lambda \end{vmatrix} \tag{5}$$

$$= (-\beta I^* - \Lambda) \begin{vmatrix} \beta S^* - \gamma - \Lambda & 0 \\ \gamma & 0 - \Lambda \end{vmatrix} - (-\beta S^*) \begin{vmatrix} \beta I^* & 0 \\ 0 & 0 - \Lambda \end{vmatrix} + 0 \begin{vmatrix} \beta I^* & \beta S^* - \gamma - \Lambda \\ 0 & \gamma \end{vmatrix} \tag{6}$$

$$= (-\beta I^* - \Lambda)(\beta S^* - \gamma - \Lambda)(-\Lambda) + \beta S^* \beta I^* (-\Lambda) \tag{7}$$

Substituting in the S^* and I^* values for the disease-free equilibrium, $S^* = 1$ and $I^* = 0$, leaves:

$$(-\beta \times 0 - \Lambda)(\beta \times 1 - \gamma - \Lambda) + \beta(1)\beta(0)(-\Lambda) \tag{8}$$

$$= -\Lambda(\beta - \gamma - \Lambda) \tag{9}$$

Roots occur at $\Lambda = 0$ and $\Lambda = \beta - \gamma$. The latter solution is the epidemic growth rate.

2.1 Tau-leap implementation of stochastic movement

We use a tau-leap algorithm to simulate cell-to-cell movement by reservoir hosts. The tau-leap is a two-step approximation that extends the Gillespie algorithm to operate on discrete and systematic units of time, Δt, while also allowing

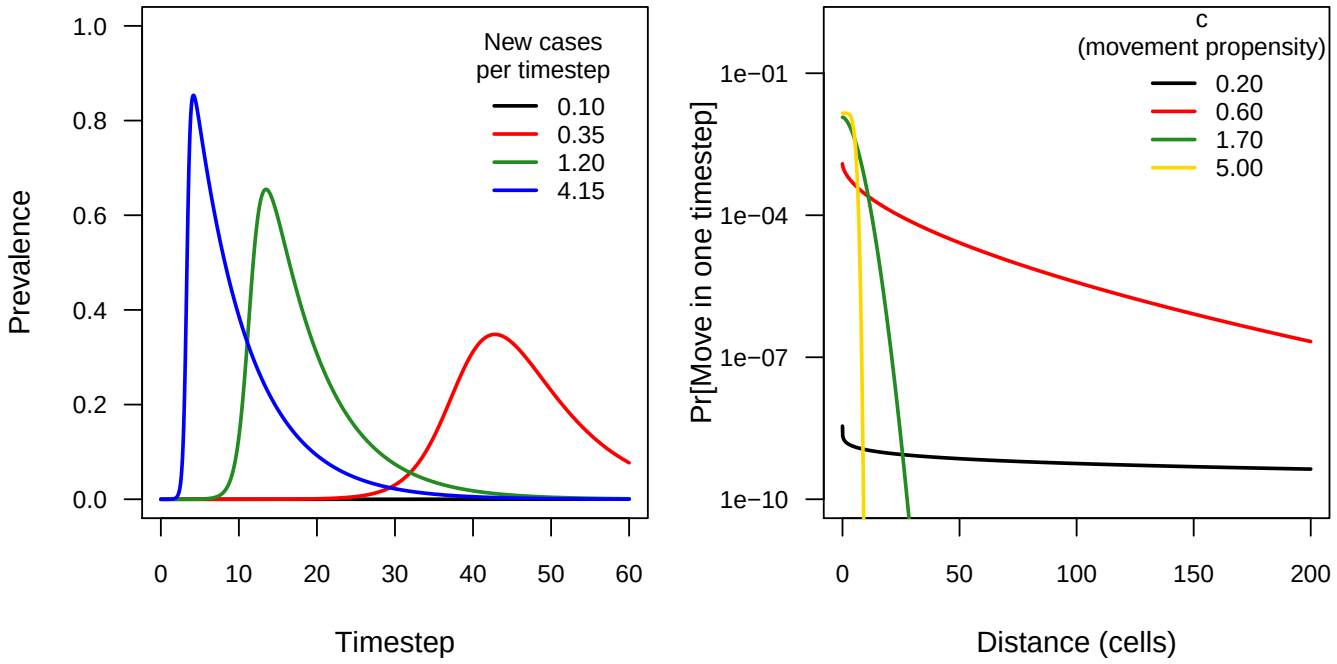

Figure S1: A) Disease dynamics under the range of epidemic growth rates explored here. B) Dispersal kernels under the range of c-values explored here. Note that the tailweight declines as c increases.

updates to occur in blocks (this is a useful feature in our scenario, since we are interested in a timescale where waiting times between moves are quite low, such that simulating waits between specific moves is computationally impractical). The first step of the tau-leap is to draw the number of moves during Δt, $N_{\text{events}}(\Delta t)$, from a Poisson distribution, such that

$$N_{\text{events}}(\Delta t) \sim \text{Poisson}\left(\lambda\right), \tag{10}$$

$$\lambda = \sum_{i,j} \text{move}_{ij} \tag{11}$$

The second step is to then draw the originating and terminal cells associated with each move, Connect(Δt), generated by a draw of size $N_{\text{events}}(t)$ from a multinomial distribution with probabilities equal to p_{ij}.

$$\text{Connect}_1(\Delta t) \sim \text{Multinom}\left(N_{\text{events}}(\Delta t), p_{ij}\right) \tag{12}$$

$$\tag{13}$$

Because this is a multinomial draw, several moves between the same pair of cells can occur within a single unit of time; the frequency of moves remains in proportion to the pairwise distance between cells. We assume that $p_{ij} = p_{ji}$, though this would not necessarily be the case. Thus, after drawing the pair of connected cells, we then assign a direction to

all moves using a single of draw of size $N_{\text{events}}(\Delta t)$, from a binomial distribution with success probability of .5.

$$\text{Direction}(\Delta t) \sim \text{Binomial}\left(N_{\text{events}}(\Delta t), .5\right), \tag{14}$$

$$\text{Connect}(\Delta t)[i] = \begin{cases} \text{Connect}_1(\Delta t)[i] & \text{if Direction}(\Delta t)[i] = 0, \\ \text{rev}(\text{Connect}_1(\Delta t)) & \text{otherwise} \end{cases} \tag{15}$$

Once the originating cells are determined, we then simulate the infection status of the moving host, which is determined by a Bernoulli trial associated with each move in Connect(Δt), with success probabilities defined by the current prevalence (number of infectious individuals) present in each connection's originating cell. Prevalence is in turn determined by identifying the current "infection age" of the originating cell (that is, the difference between current time and time at which the cell was first infected), and solving for I in the equations 1-3 at that infection age.

This progression of events produces a stochastically determined set of moves, with every move assigned a corresponding binary infection status (infectious or not). Any movement of an infectious host initiates the deterministic disease transmission process in the terminal cell. Throughout the simulation, we assume cell-specific population sizes remain constant, and we assume that cell-to-cell movement probabilities do not change throughout the simulation.

2.2 Tail weight in the dispersal function

In order to modulate the movement distribution, we used a family of dispersal kernel distributions that could range from exponential to leptokurtic (i.e., fat-tailed [17,18]). This flexibility is important, since well-characterized dispersal kernels for animal species vary, but are often heavy-tailed (e.g., [19, 20]). Let $f\left(\text{dist}_{ij}\right)$ be the dispersal probability between two points at a fixed distance dist_{ij}. Then

$$f\left(\text{dist}_{ij}\right) = \frac{1}{N}\exp\left[-\left(\frac{\text{dist}_{ij}}{\alpha}\right)^c\right]$$

In this formulation, α is a parameter describing the dispersal distance, c is a shape parameter controlling the distribution's kurtosis, and N is a normalization constant that can be written as

$$N = \frac{2\pi\alpha^2\Gamma\left(\frac{2}{c}\right)}{c}$$

where $\Gamma(x)$ is the usual Γ function. For $c \leq 1$, the distribution is fat-tailed; it is exponential at $c = 1$, and platykurtic at $c > 1$ (for reference, the Gaussian distribution has c = 2). Cell-to-cell movement probabilities, p_{ij}, are proportional to dist_{ij}, normalized across all potential moves. We rescale the weights of all distributions so that the total number of expected moves is held constant across all values of c. Dispersal is taken to be symmetric in all directions.

2.3 Implementation of management actions

2.3.1 Prophylactic vaccination

Both forms of vaccination work primarily on the deterministic side of the disease transmission model, by effectively lowering the disease's R_0 value ($p_c = 1 - \frac{1}{R_0}$) [3]. Prophylactic vaccination operates prior to spillover, and alters the proportion of susceptible hosts. We simulate prophylactic vaccination by shifting the initial conditions for the transmission process, so that some proportion of the host population starts in the "recovered", as opposed to "susceptible", state. Prophylactic vaccination is applied at a constant rate (equal to the proportion require to achieve herd immunity based on the system's R_0) across all occupied host cells over the entire spatial domain. This strategy is being used in an effort to manage spillover risk for avian influenza and rabies. We explore its implications when applied to either the reservoir or the recipient host species.

2.3.2 Retroactive vaccination

Retroactive vaccination consists of responsively vaccinating hosts in reaction to pathogen detection. In our simulation, this is mathematically identical to prophylactic vaccination (some proportion of the susceptible recipients are shifted to the recovered category), but instead of vaccinating all premises to the same level, we vaccinate only the patches in which the infection itself reaches a predetermined threshold, and those patches' direct neighbors. Vaccination is applied at the proportion required to achieve herd immunity, as determined by R_0. Retroactive vaccination can be applied to either the reservoir or the recipient host. Retroactive vaccination does not completely eliminate the pathogen.

2.3.3 Contact biosecurity

Contact biosecurity consists of actions like improving fencing and removing attractants, and aims to reduce the rate of direct contacts between the reservoir and the recipient hosts in the same patch. We simulate contact biosecurity actions by reducing the probability of interspecific contacts by a fixed constant in patches where "biosecurity" is applied. As with retroactive vaccination, biosecurity is applied when pathogen prevalence crosses a pre-specified threshold in the reservoir host. We take biosecurity to reduce the interspecific contact rate by 90% in all simulations here.

2.3.4 Selective removal

selective removal strategies alter disease transmission by reducing prevalence in the reservoir host population. This strategy has been tested, for example, to manage brucellosis in elk in parts of Wyoming (Scurlock report), and to improve bighorn sheep population growth rates following disease spillover events. We simulate selective removal by reducing reservoir host prevalence in targeted patches by a particular amount - that is, the proportion of reservoir hosts in the infected category is lowered. This affects the deterministic disease dynamics. Isolation and removal of symptomatic individuals is a special case of selective removal, with no testing cost. Here, we only apply selective removal to the reservoir host.

2.3.5 Depopulation

Depopulation consists of complete removal of all animals of the specified host species from a given cell and its neighbors within the management radius. Depopulation is followed by instantaneous restocking of all depopulated cells with susceptible hosts, so it has no effect on cell density. This is a reasonable assumption if spillover events do not lead to massive, species-wide reductions in host densities.

2.3.6 Containment

Under the containment strategy, we first identify all cells within a fixed distance of the epidemic's starting point. Since disease is deterministic in this model, cells where the epidemic begins will always cross the prevalence detection threshold first, so the initiating cells are the same as the cells where infection is first detected. We then group the cells into a community of cells within the "containment" zone, and a community of cells outside that zone. We completely eliminated all moves between the two groups for both the recipient and the reservoir host populations.

3 Parameters and parameter space explored

The simulator has 17 parameters, six of which we varied systematically in our simulation study. A complete list of all parameters is included in Table S2. We systematically varied the six investigated parameters in a full-factorial design, and ran a replicate simulation at each combination.

Parameter	Description	# levels	Values investigated
β	Determines epidemic growth rate (expected # new cases per day)	4	0.10, 0.34, 1.20, 4.14
c	Dispersion parameter of movement kernel	4	0.20, 0.58, 1.71, 5.00
γ	Recovery rate	1	1/7
Management	Management action implemented	9	Depopulation of the reservoir Depopulation of the recipient Prophylactic vaccination of the reservoir Prophylactic vaccination of the recipient Biosecurity Selective removal Retroactive vaccination of the reservoir Retroactive vaccination of the recipient Containment None
N	Size of the reservoir host population within each cell	4	10, 368, 13572, 500,000
$\tau_{\max}$	Number of timesteps simulation ran	1	60
X_{in} and Y_{in}	$X-$ and $Y-$ dimensions of the grid defining the simulator's spatial extent	1	50
ξ	Spatial radius defining the neighborhood of cells $\mathbf{A}$ within which management is applied	1	3
ψ	Biosecurity efficacy from Table S2 above	1	0.1
ν	Proportion of individuals in a cell who receive prophylactic vaccination	1	$1 - \frac{1}{R_0}$
θ	Prevalence that initiates management	4	0.001, 0.01, 0.10, 1.00
Spatial divide	Distance (number of cells) between population centroids of reservoir and recipient host populations	4	0, 15, 30, 45
ι	Containment distance	1	1/10,000
Interspecific contact rate	Interspecific contact rate	1	Within-species contact rate between cells 2 units apart according to the specified movement kernel
Premise size	Number of animals of the recipient host species per occupied cell	1	N
ρ	Multiplicative constant adjusting the weighting in the movement kernel to generate an appropriate number of moves	1	10,000
α	Term structuring the dispersal kernel	1	5

Table S2: Parameters that were systematically varied during the simulations, along with values investigated. Simulations presented in main text figures were run on a finer grid of twenty partitions each along c and epidemic growth rate.

4 Assessing model performance

We assessed model performance visually under a wide range of parameter combinations to be sure the simulator performed as expected. We first evaluated whether our spatial configuration protocol worked properly by plotting occupancy patterns for the reservoir and recipient host under varying levels of spatial divide (Figure S2).

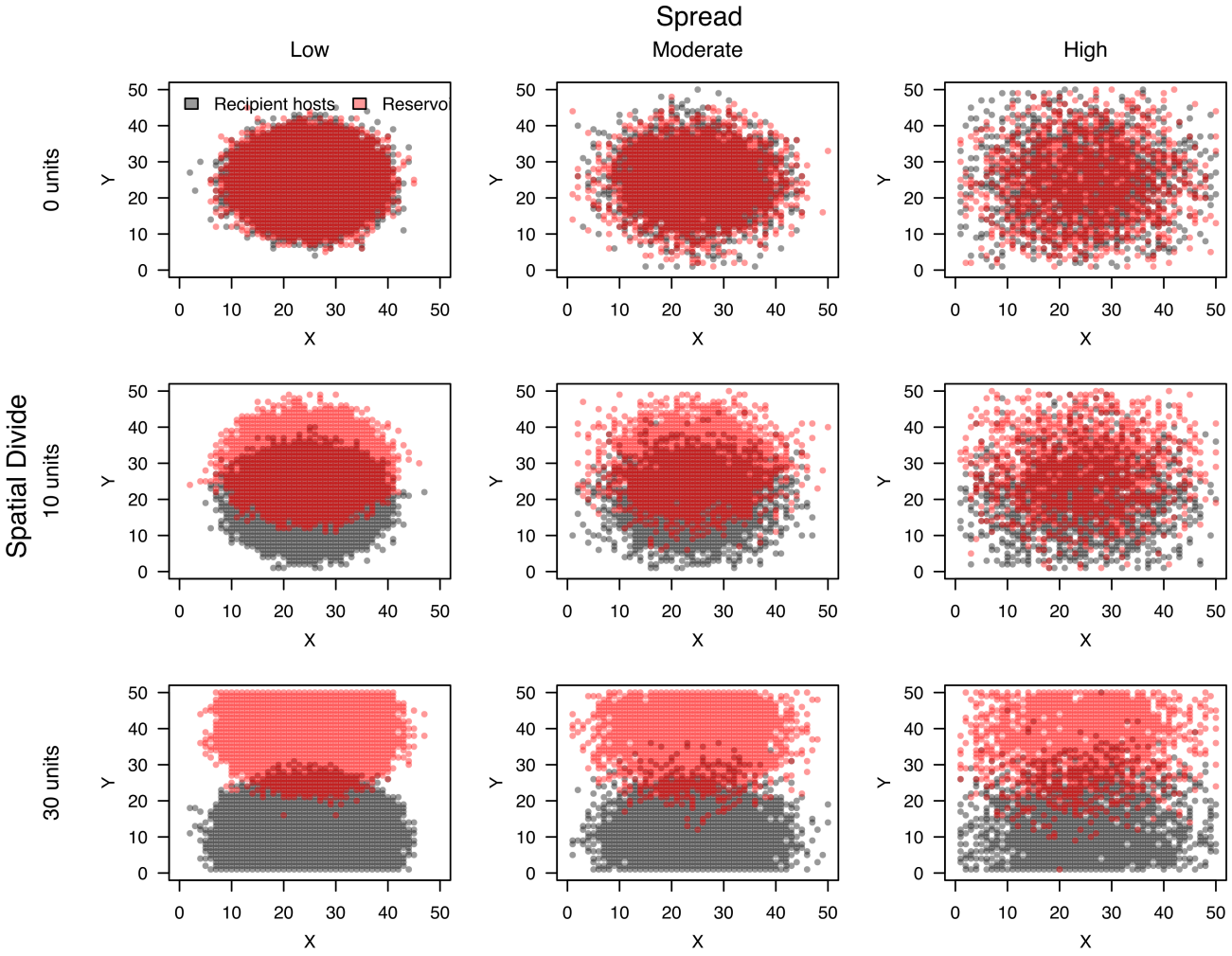

Figure S2: Spatial configurations of reservoir and recipient hosts under different values of "spread" and "spatial divide".

We then plotted reservoir and recipient host epidemic dynamics across a systematic grid of the movement kernel and epidemic growth rate space to confirm that the simulator achieved a wide range of epidemic structures (Figure S3). As anticipated, epidemics spread to many cells, quickly, in unmanaged scenarios with high β-values. This growth occurred as a clear propagating process away from the location of the index cases when host movement propensities were low (which is to say, c-values in the dispersal kernel function were high), but spread rapidly throughout the entire simulation space when host movement propensities were high (which is to say, c-values were low).

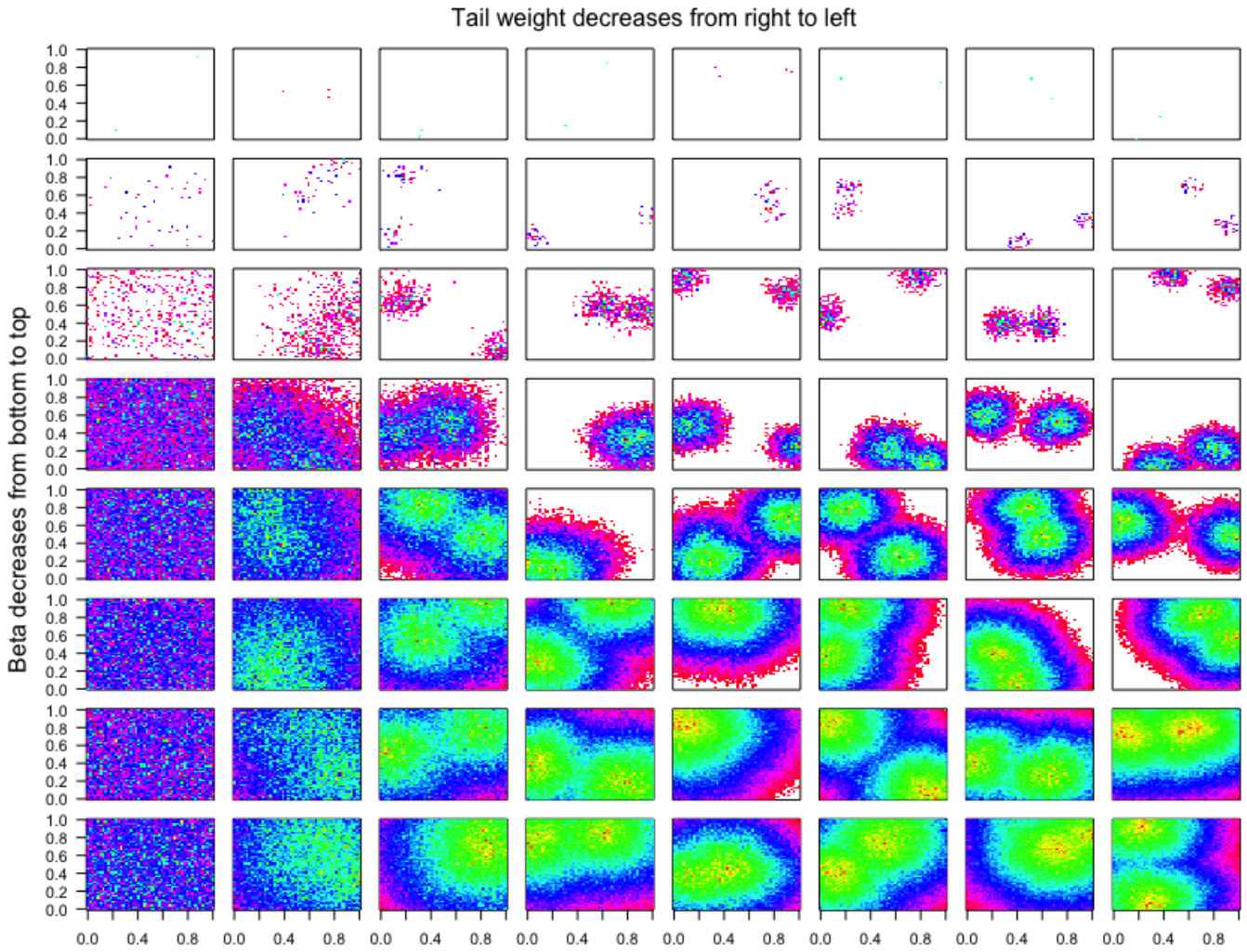

Figure S3: Spatial maps of simulated pandemics in the reservoir host, in the absence of management. Dimensions within individual plots are two-dimensional pictures of space (i.e., "latitude" and "longitude"). Cell colors reflect the first timestep that cell was infected, with the center red point being the initiating cells, ranging through yellow (earliest) to fuschia (last infected). .

We quantified the spatial configuration of each epidemic within the reservoir host more explicitly to be sure spatial propagation was operating as intended. At the end of the simulation, we categorized all cells as ever experiencing infection during the simulation (cells were assigned a 1 if they became infected at any time during the simulation, and 0 otherwise). We then removed all uninfected cells, and constructed a spatial network of infected cells, in which cells were connected to their direct spatial neighbors. This gave us a transmission network (albeit an undirected one). We calculated the number of components (isolated groups of contiguous, infected cells) and the maximum component size in the transmission network to determine how many isolated patches became infected over the course of the epidemic. Number of components gave us a coarse metric of the epidemic's fragmentation over the landscape. This same protocol was also adopted for recipient host cells. We then examined propagation dynamics in the reservoir to be sure that the epidemic was more likely to create a giant connected component when c was high (i.e., host movement propensities were low), but disaggregated into multiple small epicenters of infection when c was low (i.e., host movement propensities

were high; Figure S4).

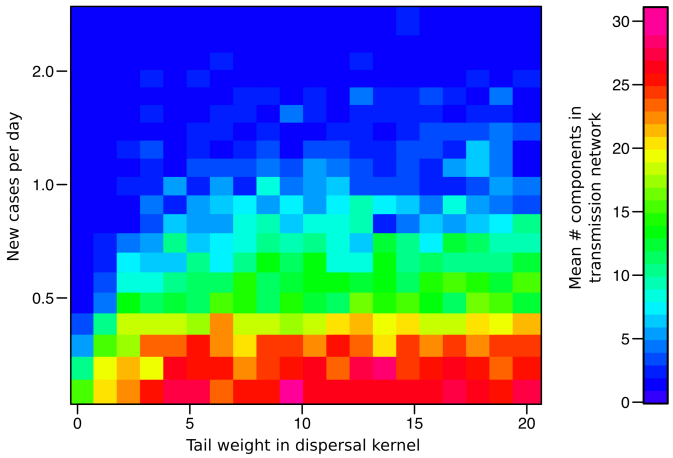

Figure S4: Phase transitions in wave dynamics. Transmission modulates between occurrence within a giant connected component (blue) and occurrence across dispersed, spatially disjoint epidemics (red) over our two-dimensional parameter space in the reservoir host. Consistent with previous work [21], the patterns indicate that the threshold value for widespread spatial transmission regularly exceeds the conventionally accepted $R_0 = 1$ threshold. This is because contact processes dominated by local contacts quickly become saturated, so that the assumption a "completely susceptible population" is rapidly invalid [22].

We visually assessed the performance of each management action at a few cross-sections of the disease parameter space. An example containing the visualization for high-R_0 ($\beta = 4.825$) and moderate c are shown in the Main Text (Figure 2), but we show dynamics under a more complete cross section of epidemic growth rates and movement propensities in Figure S3.

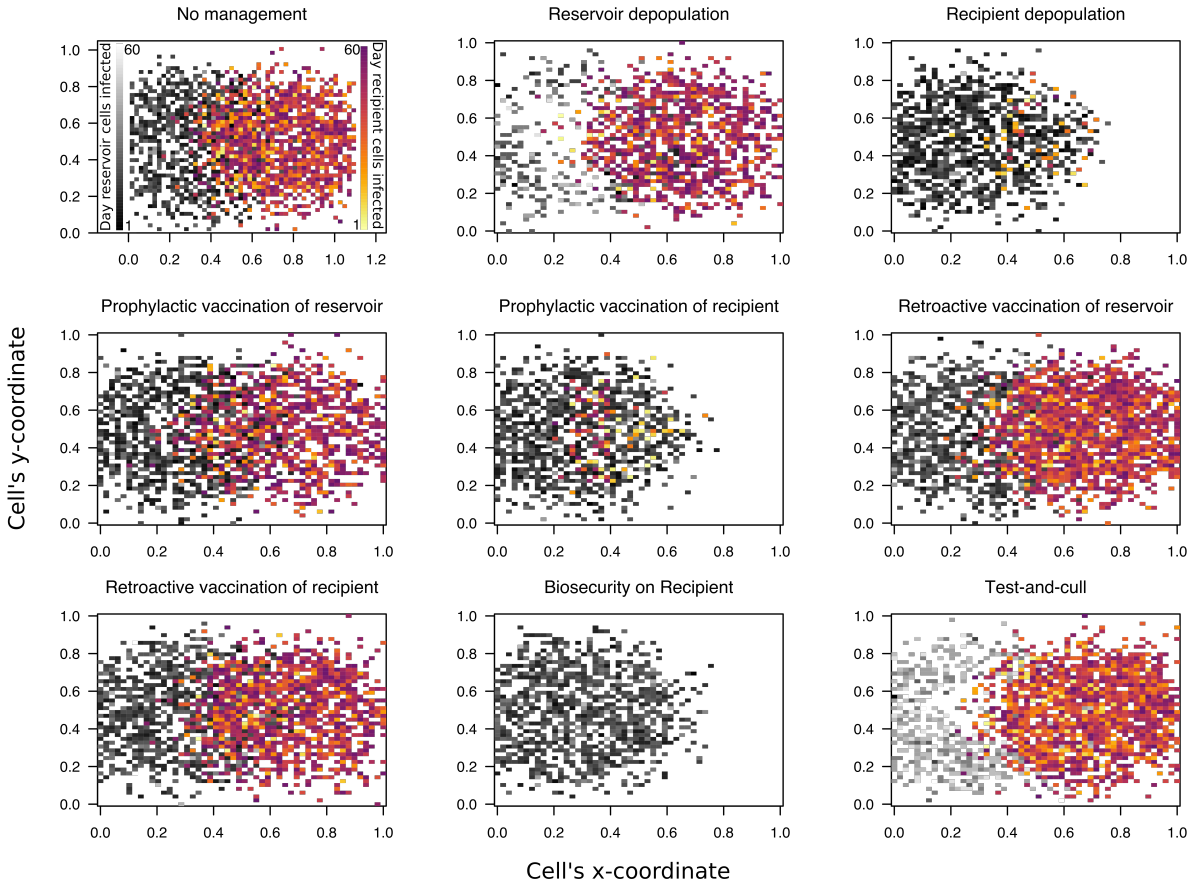

Figure S5: Different management actions simulated on a common disease propagation space.

5 Additional results

5.1 Additional specifications for simulations in Figure 4

All fits used for Figure 4 in the main text were generated from models that also included a term for spatial divide between reservoir and recipient host activity centers. Complete model results are included in the Supplementary Materials: Section 5.2. Simulations in panels A-D partition both epidemic growth rate and c into 20 blocks, fix management initiation prevalence to 0.01, and set the spatial divide between host activity centers to 30 cells.

5.2 Aggregate performance of the management actions

Table 3 shows aggregate performance of each management actions across the entire disease propagation space.

Objective	Action	% "best"
Minimise recipient patches	Biosecurity	0.19
	Depopulation of the Recipient	0.05
	Depopulation of the Reservoir	0.07
	Prophylactic Vaccination of the Recipient	0.06
	Prophylactic Vaccination of the Reservoir	0.13
	Retroactive vaccination of the Reservoir	0.19
	Retroactive vaccination of the Recipient	0.19
	Containment	0.06
	Selective removal of the reservoir	0.05
Minimise recipient prevalence	Biosecurity	0.18
	Depopulation of the Recipient	0.07
	Depopulation of the Reservoir	0.07
	Prophylactic Vaccination of the Recipient	0.07
	Prophylactic Vaccination of the Reservoir	0.14
	Retroactive vaccination of the Reservoir	0.18
	Retroactive vaccination of the Recipient	0.18
	Containment	0.06
	Selective removal of the reservoir	0.05
Minimise reservoir patches	Biosecurity	0.01
	Depopulation of the Recipientp	0.01
	Depopulation of the Reservoir	0.05
	Prophylactic Vaccination of the Recipient	0.02
	Prophylactic Vaccination of the Reservoir	0.55
	Retroactive vaccination of the Reservoir	0.26
	Retroactive vaccination of the Recipient	0.01
	Containment	0.01
	Selective removal of the reservoir	0.09
Minimise reservoir prevalence	Biosecurity	0.15
	Depopulation of the Recipient	0.15
	Depopulation of the Reservoir	0.06
	Prophylactic Vaccination of the Recipient	0.17
	Prophylactic Vaccination of the Reservoir	0.01
	Retroactive vaccination of the Reservoir	0.02
	Retroactive vaccination of the Recipient	0.13
	Containment	0.15
	Selective removal of the reservoir	0.15

Table S3: Proportion of time each management action performed "best" under each objective, across the entire range of epidemic growth rates and host movement propensities explored here.

5.3 Logistic regression model fits

Table S4: Coefficient estimates from logistic regression models describing scenarios where biosecurity outperformed all other management actions (coded as 1) vs. scenarios where biosecurity was outperformed by other actions (coded as 0). We show coefficient estimates associated with models fit to each of four measured objective metrics: minimum recipient patches, minimum recipient prevalence, minimum reservoir patches, and minimum reservoir prevalence. In all cases, the model was: $(Y) = \beta_0 + \beta_1 \ln(\beta) + \beta_2 \ln(c) + \beta_3 (\ln(\beta) : \ln(c))$, where Y represents the particular objective metric employed.

	Dependent variable:			
	I(Biosecurity was most effective management action) for each of the following:			
	(Min. recip. patches)	(Min. recip. prev.)	(Min. reserv. patches)	(Min. reserv. prev.)
$\ln(\beta)$	0.133^{*}	0.079	-0.116	-0.027
	(0.074)	(0.074)	(0.624)	(0.193)
$\ln(c)$	-0.209^{***}	-0.148^{**}	0.065	0.234
	(0.068)	(0.067)	(0.483)	(0.180)
$\ln(\beta)$:$\ln(c)$	-0.171^{***}	-0.124^{**}	0.315	0.095
	(0.064)	(0.063)	(0.528)	(0.157)
Constant	-1.748^{***}	-1.821^{***}	-3.442^{***}	-2.001^{***}
	(0.079)	(0.078)	(0.564)	(0.218)
Observations	1,365	1,418	126	220
Log Likelihood	-546.496	-558.162	-17.450	-80.997
Akaike Inf. Crit.	1,100.993	1,124.325	42.899	169.995

Note: Columns contain coefficient estimates (standard errors) for each coefficient in the model corresponding to the column's label.
*p<0.1; **p<0.05; ***p<0.01

Table S5: Coefficient estimates from logistic regression models describing scenarios where retroactive vaccination of the reservoir host outperformed all other management actions (coded as 1) vs. scenarios where retroactive vaccination of the reservoir host was outperformed by other actions (coded as 0). We show coefficient estimates associated with models fit to each of four measured objective metrics: minimum recipient patches, minimum recipient prevalence, minimum reservoir patches, and minimum reservoir prevalence. In all cases, the model was: $(Y) = \beta_0 + \beta_1 \ln(\beta) + \beta_2 \ln(c) + \beta_3 (\ln(\beta) : \ln(c))$, where Y represents the particular objective metric employed.

	Dependent variable:			
	I(Retroactive vaccination was most effective management action) for each of the following: I(Biosecurity was most effective management action) for each of the following:			
	(Min. recip. patches)	(Min. recip. prev.)	(Min. reserv. patches)	(Min. reserv. prev.)
$\ln(\beta)$	0.129^{*}	0.076	-0.645	-3.036^{**}
	(0.074)	(0.074)	(0.543)	(1.537)
$\ln(c)$	-0.216^{***}	-0.154^{**}	0.126	-0.828
	(0.068)	(0.067)	(0.359)	(1.616)
$\ln(\beta)$:$\ln(c)$	-0.168^{***}	-0.121^{*}	0.073	-0.791
	(0.064)	(0.063)	(0.462)	(1.177)
Constant	-1.742^{***}	-1.816^{***}	-2.886^{***}	-6.310^{***}
	(0.079)	(0.078)	(0.426)	(2.108)
Observations	1,365	1,418	126	220
Log Likelihood	-548.188	-559.934	-23.271	-31.717
Akaike Inf. Crit.	1,104.376	1,127.869	54.543	71.434

Note: Columns contain coefficient estimates (standard errors) for each coefficient in the model corresponding to the column's label.
*p<0.1; **p<0.05; ***p<0.01

Table S6: Coefficient estimates from logistic regression models describing scenarios where prophylactic vaccination of the reservoir host outperformed all other management actions (coded as 1) vs. scenarios where prophylactic vaccination of the reservoir host was outperformed by other actions (coded as 0). We show coefficient estimates associated with models fit to each of four measured objective metrics: minimum recipient patches, minimum recipient prevalence, minimum reservoir patches, and minimum reservoir prevalence. In all cases, the model was: $(Y) = \beta_0 + \beta_1 \ln(\beta) + \beta_2 \ln(c) + \beta_3 (\ln(\beta) : \ln(c))$, where Y represents the particular objective metric employed.

	Dependent variable:			
	I(Prophylactic vaccination was most effective management action) for each of the following:			
	(Min. recipient patches)	(Min. recipient prevalence)	(Min. reservoir patches)	(Min. reservoir prevalence)
$\ln(\beta)$	-0.158^{**}	-0.133^{**}	0.121	0.234^{*}
	(0.066)	(0.063)	(0.208)	(0.141)
$\ln(c)$	0.071	0.048	0.026	0.098
	(0.059)	(0.056)	(0.169)	(0.131)
$\ln(\beta)$:$\ln(c)$	0.066	0.044	-0.003	-0.008
	(0.055)	(0.053)	(0.180)	(0.116)
Constant	-1.244^{***}	-1.215^{***}	-0.017	-1.086^{***}
	(0.071)	(0.066)	(0.197)	(0.159)
Observations	1,365	1,418	126	220
Log Likelihood	-740.106	-771.601	-87.139	-120.961
Akaike Inf. Crit.	1,488.211	1,551.201	182.277	249.923

Note: Columns contain coefficient estimates (standard errors) for each coefficient in the model corresponding to the column's label.
*p<0.1; **p<0.05; ***p<0.01

Table S7: Coefficient estimates from logistic regression models describing scenarios where prophylactic vaccination of the recipient host outperformed all other management actions (coded as 1) vs. scenarios where prophylactic vaccination of the recipient host was outperformed by other actions (coded as 0). We show coefficient estimates associated with models fit to each of four measured objective metrics: minimum recipient patches, minimum recipient prevalence, minimum reservoir patches, and minimum reservoir prevalence. In all cases, the model was: $(Y) = \beta_0 + \beta_1 \ln(\beta) + \beta_2 \ln(c) + \beta_3 (\ln(\beta) : \ln(c))$, where Y represents the particular objective metric employed.

	Dependent variable:			
	I(Prophylactic vaccination was most effective management action) for each of the following:			
	(Min. recipient patches)	(Min. recipient prevalence)	(Min. reservoir patches)	(Min. reservoir prevalence)
$\ln(\beta)$	-0.335^{***}	-0.215^{**}	-0.045	0.293^{*}
	(0.103)	(0.089)	(0.498)	(0.163)
$\ln(c)$	0.239^{***}	0.133^{*}	-0.235	0.007
	(0.091)	(0.079)	(0.408)	(0.152)
$\ln(\beta)$:$\ln(c)$	0.211^{**}	0.118	0.239	-0.047
	(0.083)	(0.074)	(0.434)	(0.134)
Constant	-2.299^{***}	-2.161^{***}	-3.011^{***}	-1.598^{***}
	(0.113)	(0.095)	(0.474)	(0.184)
Observations	1,365	1,418	126	220
Log Likelihood	-462.839	-493.635	-23.883	-96.354
Akaike Inf. Crit.	933.678	995.271	55.767	200.708

Note: Columns contain coefficient estimates (standard errors) for each coefficient in the model corresponding to the column's label.
*p<0.1; **p<0.05; ***p<0.01

Table S8: Coefficient estimates from logistic regression models describing scenarios where depopulation of the reservoir host outperformed all other management actions (coded as 1) vs. scenarios where depopulation of the reservoir host was outperformed by other actions (coded as 0). We show coefficient estimates associated with models fit to each of four measured objective metrics: minimum recipient patches, minimum recipient prevalence, minimum reservoir patches, and minimum reservoir prevalence. In all cases, the model was: $(Y) = \beta_0 + \beta_1 \ln(\beta) + \beta_2 \ln(c) + \beta_3 (\ln(\beta) : \ln(c))$, where Y represents the particular objective metric employed.

	Dependent variable:			
	I(Depopulation of the reservoir was most effective management action) for each of the following:			
	(Min. recipient patches)	(Min. recipient prevalence)	(Min. reservoir patches)	(Min. reservoir prevalence)
$\ln(\beta)$	0.253^{**}	0.273^{***}	0.961^{***}	-0.497^{**}
	(0.101)	(0.096)	(0.362)	(0.249)
$\ln(c)$	0.117	0.081	-0.222	-0.051
	(0.092)	(0.086)	(0.345)	(0.239)
$\ln(\beta)$:$\ln(c)$	0.057	0.047	-0.228	0.013
	(0.085)	(0.080)	(0.312)	(0.205)
Constant	-2.520^{***}	-2.470^{***}	-2.424^{***}	-2.485^{***}
	(0.110)	(0.103)	(0.409)	(0.287)
Observations	1,365	1,418	126	220
Log Likelihood	-364.294	-388.340	-46.255	-66.922
Akaike Inf. Crit.	736.589	784.679	100.511	141.845

Note: Columns contain coefficient estimates (standard errors) for each coefficient in the model corresponding to the column's label.
*p<0.1; **p<0.05; ***p<0.01

Table S9: Coefficient estimates from logistic regression models describing scenarios where depopulation of the recipient host outperformed all other management actions (coded as 1) vs. scenarios where depopulation of the recipient host was outperformed by other actions (coded as 0). We show coefficient estimates associated with models fit to each of four measured objective metrics: minimum recipient patches, minimum recipient prevalence, minimum reservoir patches, and minimum reservoir prevalence. In all cases, the model was: $(Y) = \beta_0 + \beta_1 \ln(\beta) + \beta_2 \ln(c) + \beta_3 (\ln(\beta) : \ln(c))$, where Y represents the particular objective metric employed.

	Dependent variable:			
	I(Depopulation of the recipient was most effective management action) for each of the following:			
	(Min. recipient patches)	(Min. recipient prevalence)	(Min. reservoir patches)	(Min. reservoir prevalence)
$\ln(\beta)$	-0.318^{***}	-0.166^{*}	-0.932^{*}	0.598^{***}
	(0.101)	(0.086)	(0.495)	(0.165)
$\ln(c)$	0.217^{**}	0.094	-0.045	0.061
	(0.089)	(0.076)	(0.310)	(0.154)
$\ln(\beta)$:$\ln(c)$	0.203^{**}	0.085	0.341	0.066
	(0.082)	(0.072)	(0.416)	(0.136)
Constant	-2.261^{***}	-2.105^{***}	-2.487^{***}	-1.530^{***}
	(0.110)	(0.091)	(0.370)	(0.186)
Observations	1,365	1,418	126	220
Log Likelihood	-469.663	-503.414	-29.918	-95.573
Akaike Inf. Crit.	947.325	1,014.828	67.835	199.146

Note: Columns contain coefficient estimates (standard errors) for each coefficient in the model corresponding to the column's label.
*p<0.1; **p<0.05; ***p<0.01

Table S10: Coefficient estimates from logistic regression models describing scenarios where selective removal of the reservoir host outperformed all other management actions (coded as 1) vs. scenarios where selective removal of the reservoir host was outperformed by other actions (coded as 0). We show coefficient estimates associated with models fit to each of four measured objective metrics: minimum recipient patches, minimum recipient prevalence, minimum reservoir patches, and minimum reservoir prevalence. In all cases, the model was: $(Y) = \beta_0 + \beta_1 \ln(\beta) + \beta_2 \ln(c) + \beta_3 (\ln(\beta) : \ln(c))$, where Y represents the particular objective metric employed.

	Dependent variable:			
	I(Selective removal was most effective management action) for each of the following:			
	(Min. recipient patches)	(Min. recipient prevalence)	(Min. reservoir patches)	(Min. reservoir prevalence)
$\ln(\beta)$	0.231^{*}	0.304^{***}	-23.835	-0.508^{**}
	(0.125)	(0.109)	(3,550.751)	(0.226)
$\ln(c)$	0.234^{**}	0.101	-10.241	0.070
	(0.111)	(0.099)	(1,578.818)	(0.216)
$\ln(\beta)$:$\ln(c)$	0.085	0.025	-14.629	0.010
	(0.102)	(0.092)	(2,206.206)	(0.186)
Constant	-2.940^{***}	-2.784^{***}	-19.767	-2.248^{***}
	(0.135)	(0.118)	(2,541.010)	(0.260)
Observations	1,365	1,418	126	220
Log Likelihood	-283.922	-316.200	-11.636	-76.913
Akaike Inf. Crit.	575.845	640.401	31.273	161.827

Note: Columns contain coefficient estimates (standard errors) for each coefficient in the model corresponding to the column's label.
*p<0.1; **p<0.05; ***p<0.01

Table S11: Coefficient estimates from logistic regression models describing scenarios where no management outperformed all other management actions (coded as 1) vs. scenarios where no management was outperformed by other actions (coded as 0). We show coefficient estimates associated with models fit to each of four measured objective metrics: minimum recipient patches, minimum recipient prevalence, minimum reservoir patches, and minimum reservoir prevalence. In all cases, the model was: $(Y) = \beta_0 + \beta_1 \ln(\beta) + \beta_2 \ln(c) + \beta_3 (\ln(\beta) : \ln(c))$, where Y represents the particular objective metric employed.

	Dependent variable:			
	I(No action was most effective management action) for each of the following:			
	(Min. recipient patches)	(Min. recipient prevalence)	(Min. reservoir patches)	(Min. reservoir prevalence)
$\ln(\beta)$	-0.341^{***}	-0.274^{***}	-0.148	0.118
	(0.104)	(0.093)	(0.518)	(0.197)
$\ln(c)$	0.249^{***}	0.180^{**}	-0.034	-0.391^{**}
	(0.092)	(0.082)	(0.401)	(0.182)
$\ln(\beta)$:$\ln(c)$	0.218^{***}	0.164^{**}	0.422	-0.151
	(0.084)	(0.076)	(0.438)	(0.159)
Constant	-2.306^{***}	-2.214^{***}	-3.027^{***}	-1.993^{***}
	(0.113)	(0.100)	(0.469)	(0.222)
Observations	1,365	1,418	126	220
Log Likelihood	-462.510	-487.198	-23.562	-80.613
Akaike Inf. Crit.	933.020	982.395	55.124	169.227

Note: Columns contain coefficient estimates (standard errors) for each coefficient in the model corresponding to the column's label.
*p<0.1; **p<0.05; ***p<0.01

5.4 Fits under other objectives

Figures S6 through S8 show results parallel to Figure 4 in the main text, but for the other three output metrics: recipient prevalence; reservoir patches infected, and reservoir prevalence.

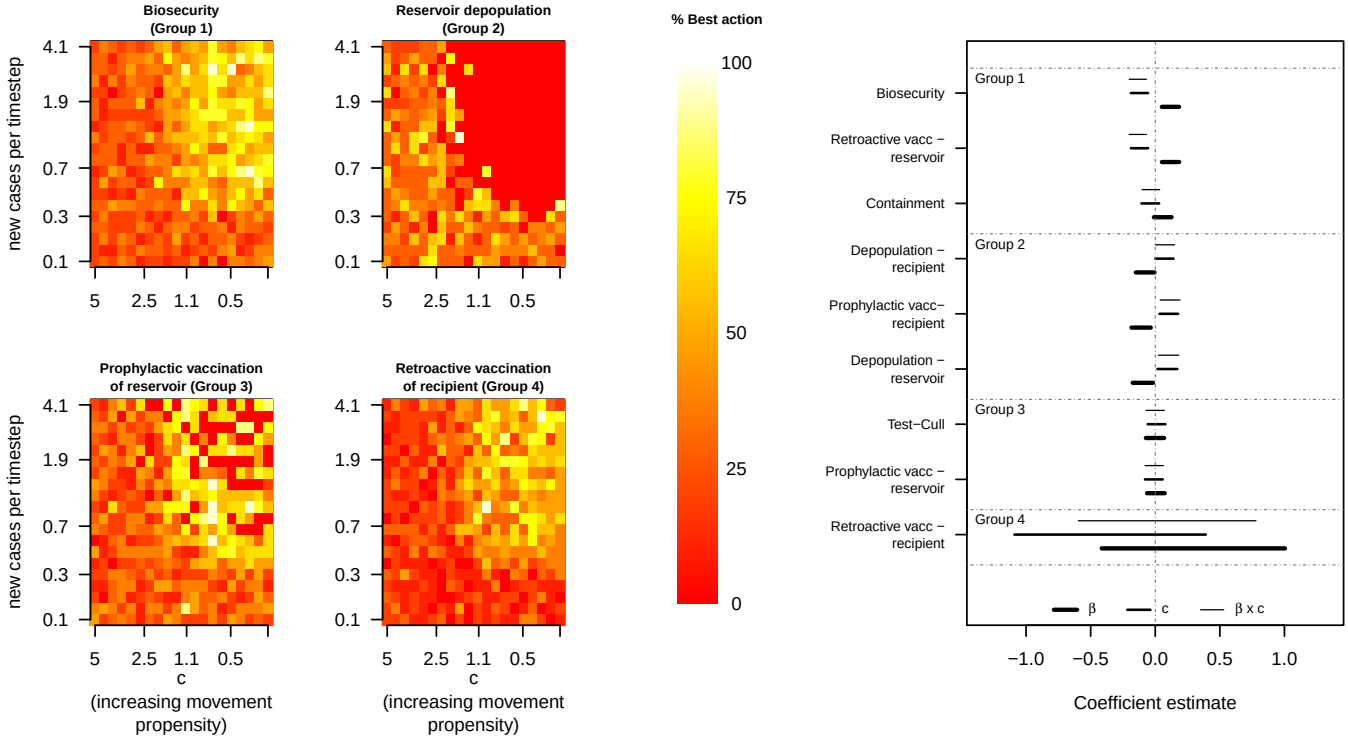

Figure S6: Relative management performance and model coefficient estimates when the response metric was the number of recipient patches infected.

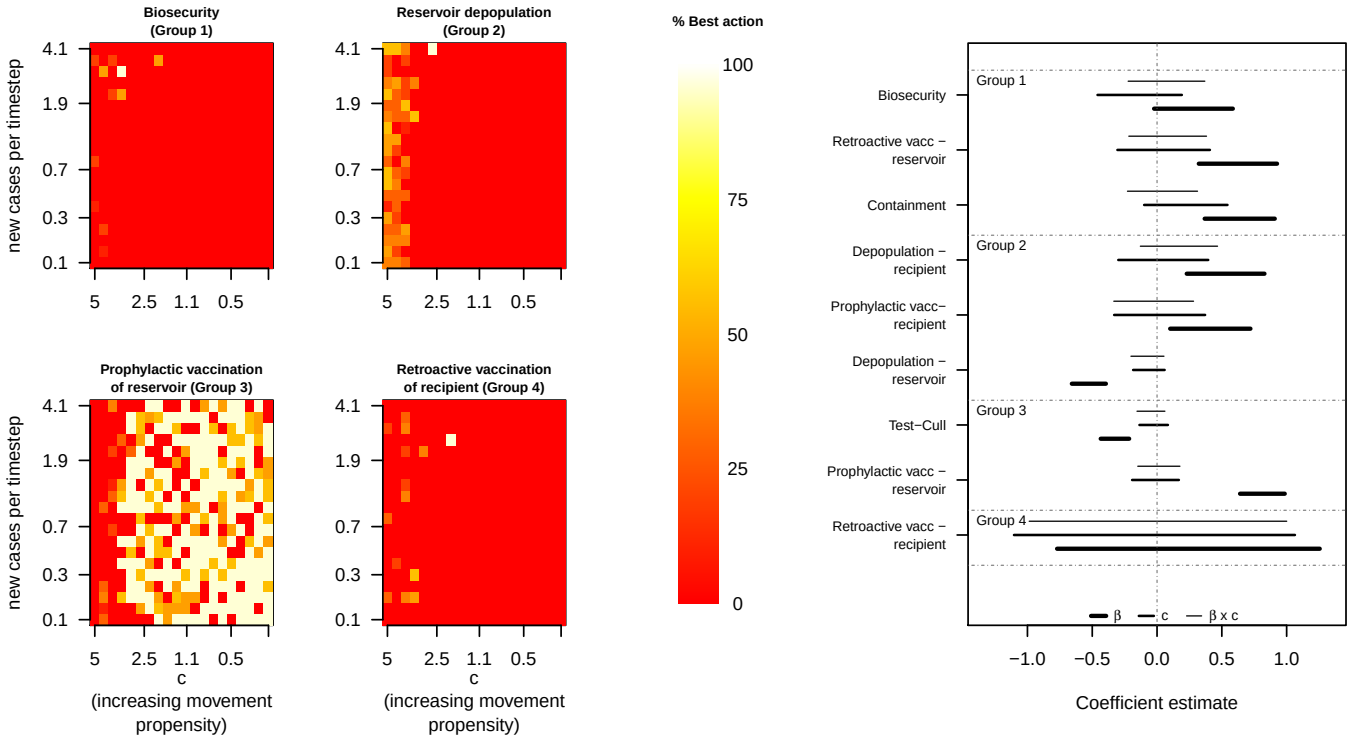

Figure S7: Management competition and model coefficient estimates when the response metric was total reservoir patches infected.

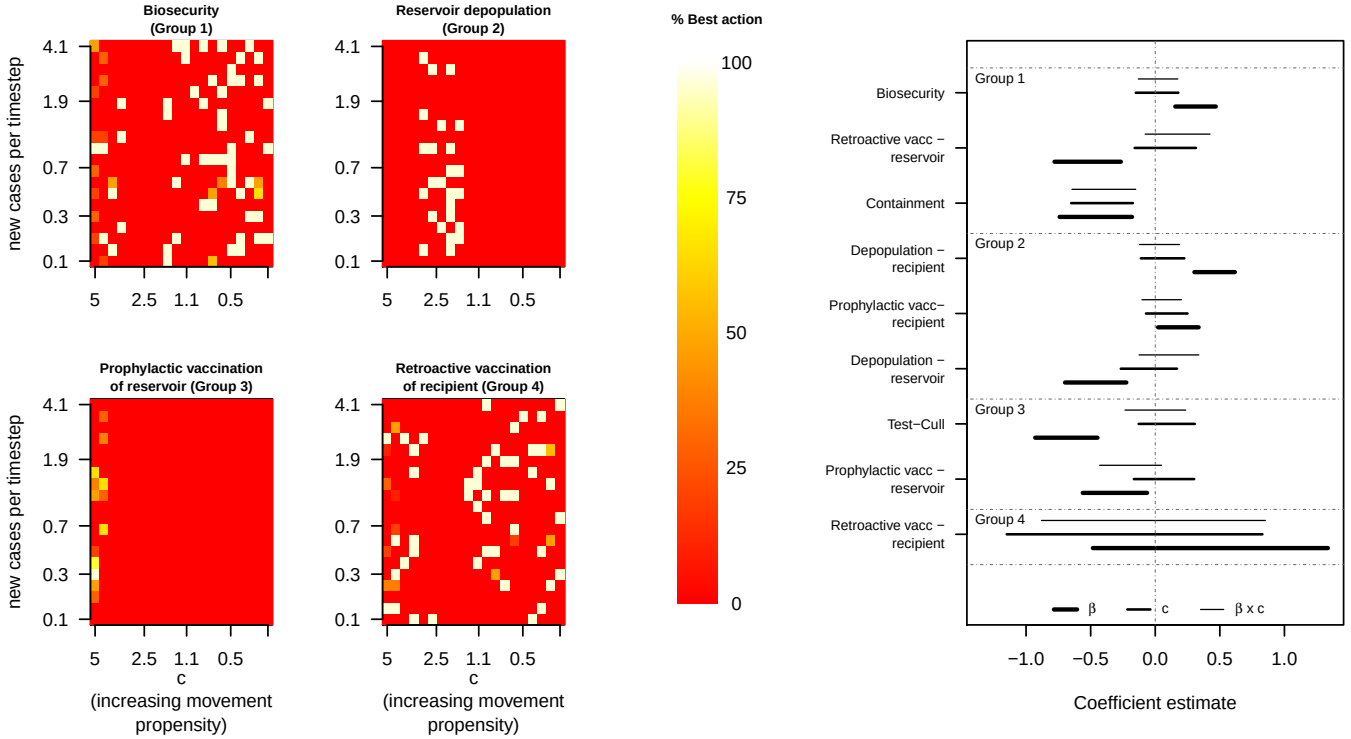

Figure S8: Management competition and model coefficient estimates when the response metric was aggregate prevalence in the reservoir host.

5.5 Classification tree approach

In addition to the logistic regression models, we also used a classification tree to to assess the role epidemic growth rate and host movement propensities played in shaping optimal management within a context where we also considered variation in spatial divide between host species, prevalence that triggered management to start, and reservoir host population densities. We fit four regression trees [23] with response values corresponding to each of our objectives (i.e., total number of recipient patches infected; maximum recipient prevalence, total number of reservoir patches infected to identify the most effective management action according to information on all six covariates. Briefly, regression trees operate by assuming a constant response model within a specified partition of the covariate space. The objective of tree-based methods is to define a path of binary splits that optimises that minimises variation in the response variable within partitions, while maximising variance among partitions. In our case, this equated to identifying covariate values at which the objective function's measured value changed substantially. The size of the trees — which is to say, the number of partitions — governs the model's complexity. We followed standard protocols of growing a very large tree, and then pruning it back to include only splits up to and including the split that minimised cross-validation error. Tree partitioning was implemented using the `rpart` package in `R` [24].

Recursive partitioning methods identify a progressive set of covariate values that best split a set of varying outcomes into groups. Once a partition is identified, subsequent partitions operate exclusively within existing groups (so that the second partitioning of one group might rely on a different covariate than the second partitioning of a different group). Once the outcomes are completely partitioned, the resulting binary tree is pruned back via cross-validation to appropriately avoid overfitting.

We used the Gini impurity criterion for the classifier, with data weights proportional to the observed frequencies of each treatment combination (this was very nearly balanced in the dataset, since we controlled the simulation's parameter space). Any risk within one standard error of the achieved minimum is marked as being equivalent to the minimum (i.e. considered to be part of the flat plateau). Then the simplest model, among all those "tied" on the plateau, is chosen.

Classifier performance was evaluated through cross-validation and trees were pruned to the complexity level associate with the minimum cross-validation error. We fit separate trees for each of four objective functions (minimizing spatial extent or prevalence in the recipient or reservoir host). Pruned trees, along with variable importance estimates in each case, are shown in Figure S7.

Variable importance from the four regression trees consistently indicated that epidemic growth rate and host movement propensities were the most important factors in determining epidemic size and spatial extent, especially when objective functions focused on the recipient host (Figure S8). Spatial separation of reservoir and recipient host activity centers and management actions were also important determinants of epidemic size and extent.

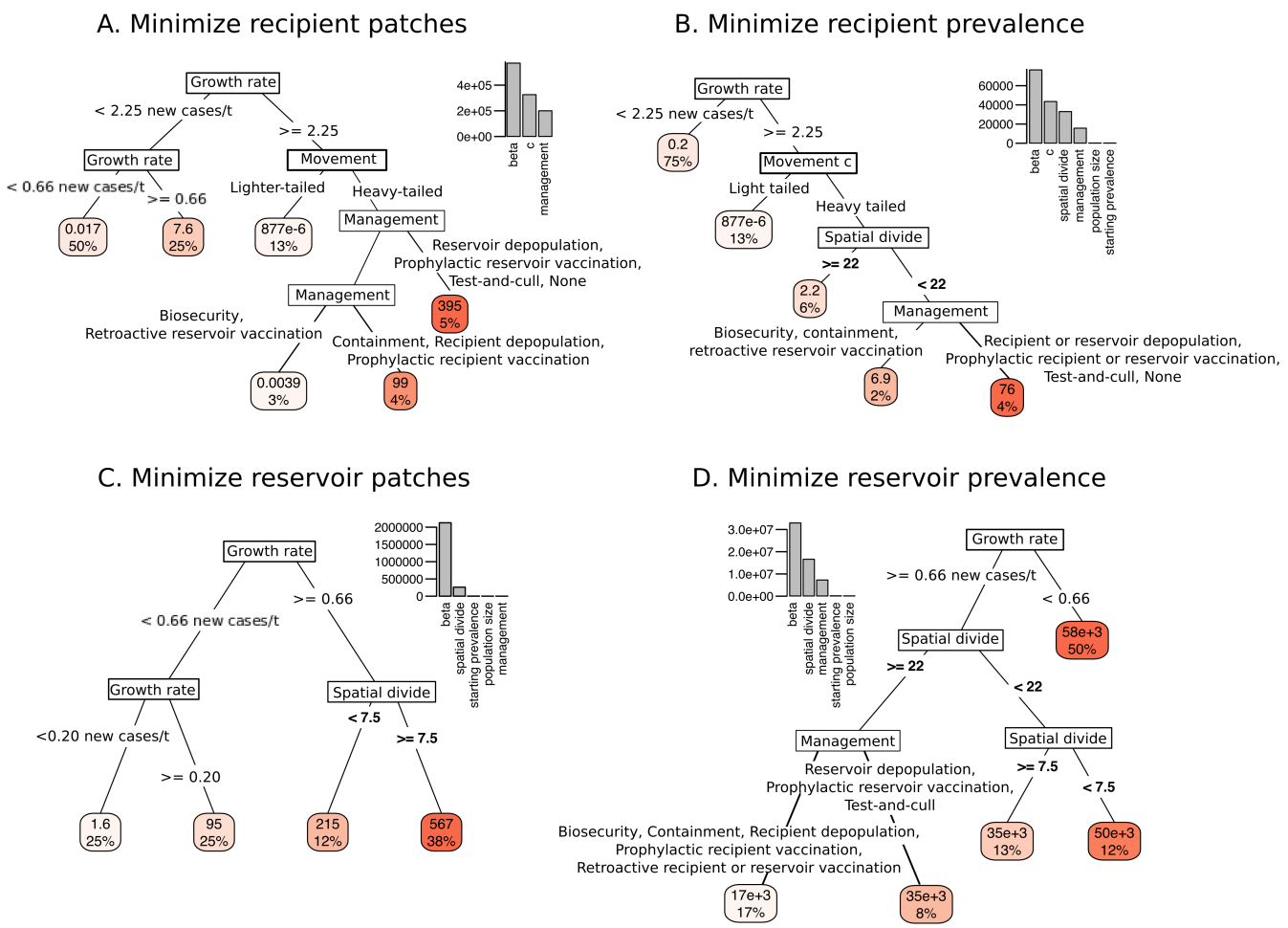

Figure S9: Regression trees showing process and management parameters associated with varying values of each of four objective functions. Leaf colors represent epidemic size (in terms of patches or prevalence), with redder leaves being larger epidemics in the specified metric. Leaf percentages reflect the total proportion of simulations landing in each leaf.

6 Limitations associated with this framework

6.1 SIR assumptions and limitations

First, commensurate with our SIR modeling structure, we assumed that any pathogen infection provided hosts with complete immunity to that pathogen in the future. However, we know this assumption is violated in several key wildlife-livestock spillover diseases (including avian influenza, leptospirosis, and bighorn sheep pneumonia, to name a few). Accounting for partial or limited cross-strain immunity would likely have slowed reservoir fade-out in the fastest-growing cases (but probably would not have lower prevalence), since epidemics would have had a larger pool of susceptible hosts available. Thus our model probably underestimates reservoir prevalence and subsequent spillover burden for diseases with partial immunity.

Second, we neglected disease-induced mortalities throughout this exploration. This might be a defensible assumption for diseases that we manage foremostly due to their downstream risks to human health (i.e., brucellosis; North

American rabies), and possibly also for diseases that pose limited consequences on reservoir host health (i.e., rabies in bats; M. ovi in domestic sheep). Limited disease induced mortality is inconsistent with many diseases of management concern at the wildlife-livestock interface. Disease-induced mortality would likely lower spillover risk in many systems for two reasons. First, mortalities curtail the duration of the infectious period, and may limit the movement potential of infected animals. Second, ill animals may be less-likely to move than their infected counterparts.

Densities would also be altered by disease-induced mortalities, and even beyond disease-related changes, many — if not most— wildlife and livestock systems in temperate latitudes exhibit seasonally pulsed densities. Varying densities would introduce additional variation into transmission rates for pathogens with density-dependent transmission routes. Decreases, and even simply oscillations in densities are thought to to drive pathogens toward local extinction however (Peel et al. 2014), so our choice to create densities as constant likely biases our model toward over-estimating spillover frequencies.

We took process parameters (per-susceptible transmission rate, recovery rate, movement rate) to be constant. but these could also feasibly change over the course of a spillover event. In the most basic case, some hosts have fundamentally different transmission parameters than others due to switches in mode of transmission that co-occur with host shifts (for instance, avian influenza's switch from primarily gastrointestinal to primarily respiratory when it switches from wild to domestic fowl). Human-mediated movement dynamics (as is especially common in livestock hosts) almost certainly change once a spillover event is detected and reported, with strong consequences on post-spillover epidemic growth rates.

6.2 Timescale and epidemic duration

We chose 60 timesteps as the duration for all simulations. This, and any other, timescale choice is somewhat arbitrary, since both epidemic dynamics and spatial movements accumulate continuously in time (though we update movements in batches; see Supplementary Materials: tau-leap). However, the 60-timestep scale aligned with our transmission, recovery, and movement rates to provide a wide range of epidemic dynamics. Additionally, it seemed reasonable that management agencies might be able to categorize pathogens as expanding on a weekly (i.e., 1 timestep), seasonal (i.e., 12 timestep), or annual (i.e., 52 timestep) scale, and to implement some management responses at a weekly scale, but probably not much faster.

6.3 Direction and independence of movements

Our simulation landscape had no structure beyond cell-to-cell distance, so distance was the only determinant of where individuals moved. Also, since we held all within-cell populations constant, there was no "crowding" effect. These assumptions are clearly violated at some level for most real-world animal systems. We also force animals to move as independent units, overlooking larger-scale migrations or group-level moves. This likely means that the number of independent movers is biased high in our simulations, but the capacity of those movers to spark an epidemic could be

biased low (since if individuals actually move in groups of 5, for example, any one of the five movers could be infected and spark an epidemic). However, without information specific to the behavioral ecology and spatial context of a given host system, we felt that adding additional detail here likely caused more problems than it alleviated.

6.4 Common movement kernels for reservoir and recipient hosts

In this simulation, we assumed that both reservoir and recipient host species moved according to identical movement kernels. This assumption was made for the purposes of simplicity, and is unlikely to hold in many wildlife-livestock situations. There are, however, a few places where it could be appropriate, and we highlight those instances here.

One context where common kernels could be reasonable is for host species that are closely related or allometrically matched (for instance, a system in which both the reservoir and the recipient host species are ungulates; a system where both hosts are canids, etc.), and both experience largely uninhibited movements (on the livestock side, this could include livestock that are ranged on grazing allotments, or animals like free-ranging domestic cats and dogs living at the urban-wildland interface).

References

[1] N Thompson Hobbs, Chris Geremia, John Treanor, Rick Wallen, PJ White, Mevin B Hooten, and Jack C Rhyan. State-space modeling to support management of brucellosis in the yellowstone bison population. *Ecological Monographs*, 85(4):525–556, 2015.

[2] Pauline L Kamath, Jeffrey T Foster, Kevin P Drees, Gordon Luikart, Christine Quance, Neil J Anderson, P Ryan Clarke, Eric K Cole, Mark L Drew, William H Edwards, et al. Genomics reveals historic and contemporary transmission dynamics of a bacterial disease among wildlife and livestock. *Nature Communications*, 7, 2016.

[3] Matt J Keeling and Pejman Rohani. *Modeling infectious diseases in humans and animals*. Princeton University Press, 2008.

[4] Valerius De Vos, Roy G Bengis, NPJ Kriek, A Michel, et al. The epidemiology of tuberculosis in free-ranging african buffalo (syncerus caffer) in the kruger national park, south africa. *The Onderstepoort Journal of Veterinary Research*, 68(2):119, 2001.

[5] PM Kitala, JJ McDermott, PG Coleman, and C Dye. Comparison of vaccination strategies for the control of dog rabies in machakos district, kenya. *Epidemiology & Infection*, 129(1):215–222, 2002.

[6] CI Cullingham, BA Pond, CJ Kyle, EE Rees, RC Rosatte, and BN White. Combining direct and indirect genetic methods to estimate dispersal for informing wildlife disease management decisions. *Molecular Ecology*, 17(22):4874–4886, 2008.

[7] Gerardo Chowell, Hiroshi Nishiura, and Luis MA Bettencourt. Comparative estimation of the reproduction number for pandemic influenza from daily case notification data. *Journal of the Royal Society Interface*, 4(12):155–166, 2007.

[8] Christina E Mills, James M Robins, and Marc Lipsitch. Transmissibility of 1918 pandemic influenza. *Nature*, 432(7019):904, 2004.

[9] Pejman Rohani, Romulus Breban, David E Stallknecht, and John M Drake. Environmental transmission of low pathogenicity avian influenza viruses and its implications for pathogen invasion. *Proceedings of the National Academy of Sciences*, 106(25):10365–10369, 2009.

[10] Robert G Webster, William J Bean, Owen T Gorman, Thomas M Chambers, and Yoshihiro Kawaoka. Evolution and ecology of influenza a viruses. *Microbiological Reviews*, 56(1):152–179, 1992.

[11] Nídia Sequeira Trovão, Marc A Suchard, Guy Baele, Marius Gilbert, and Philippe Lemey. Bayesian inference reveals host-specific contributions to the epidemic expansion of influenza a h5n1. *Molecular Biology and Evolution*, 32(12):3264–3275, 2015.

[12] Emily S Almberg, Paul C Cross, and Douglas W Smith. Persistence of canine distemper virus in the greater yellowstone ecosystem's carnivore community. *Ecological Applications*, 20(7):2058–2074, 2010.

[13] Kathleen A Alexander and Max JG Appel. African wild dogs (lycaon pictus) endangered by a canine distemper epizootic among domestic dogs near the masai mara national reserve, kenya. *Journal of Wildlife Diseases*, 30(4):481–485, 1994.

[14] Kim Murray Berger and Eric M Gese. Does interference competition with wolves limit the distribution and abundance of coyotes? *Journal of Animal Ecology*, 76(6):1075–1085, 2007.

[15] Buddhi Pantha, Judy Day, and Suzanne Lenhart. Optimal control applied in an anthrax epizootic model. *Journal of Biological Systems*, 24(04):495–517, 2016.

[16] World Health Organization et al. *Anthrax in humans and animals*. World Health Organization, 2008.

[17] James S Clark, Miles Silman, Ruth Kern, Eric Macklin, and Janneke HilleRisLambers. Seed dispersal near and far: patterns across temperate and tropical forests. *Ecology*, 80(5):1475–1494, 1999.

[18] Tom Lindström, Nina Håkansson, and Uno Wennergren. The shape of the spatial kernel and its implications for biological invasions in patchy environments. *Proceedings of the Royal Society B: Biological Sciences*, 278(1711):1564–1571, 2010.

[19] Richard J Walters, Mark Hassall, Mark G Telfer, Godfrey M Hewitt, and Jean P Palutikof. Modelling dispersal of a temperate insect in a changing climate. *Proceedings of the Royal Society B: Biological Sciences*, 273(1597):2017–2023, 2006.

[20] Andrew J Tatem, Simon I Hay, and David J Rogers. Global traffic and disease vector dispersal. *Proceedings of the National Academy of Sciences*, 103(16):6242–6247, 2006.

[21] Paul C Cross, James O Lloyd-Smith, Philip LF Johnson, and Wayne M Getz. Duelling timescales of host movement and disease recovery determine invasion of disease in structured populations. *Ecology Letters*, 8(6):587–595, 2005.

[22] Daniel J Salkeld, Marcel Salathé, Paul Stapp, and James Holland Jones. Plague outbreaks in prairie dog populations explained by percolation thresholds of alternate host abundance. *Proceedings of the National Academy of Sciences*, 107(32):14247–14250, 2010.

[23] Leo Breiman. *Classification and regression trees*. Routledge, 1984.

[24] Terry M Therneau, Beth Atkinson, and Maintainer Brian Ripley. The rpart package, 2010.